November 2017

Calibration-free Spectrophotometric Measurements of Carbonate Saturation States in Seawater

Erin E. Cuyler
University of South Florida, erincuyler@mail.usf.edu

Calibration-free Spectrophotometric Measurements of Carbonate Saturation States in Seawater

by

Erin E. Cuyler

A thesis submitted in partial fulfillment
of the requirements for the degree of
Master of Science
College of Marine Science
University of South Florida

Major Professor: Robert H. Byrne, Ph.D.
Lisa Robbins, Ph.D.
Pamela Hallock Muller, Ph.D.

Date of Approval:
October 31, 2017

Keywords: Carbon dioxide, ocean acidification, pH, coastal monitoring, spectrophotometry, marine chemistry

Dedication

To my parents, Janice and Richard Cuyler. I could not have done this without the unconditional love and support that you have given me throughout my life, thank you.

Acknowledgments

First and foremost, I would like to thank Dr. Robert Byrne for his invaluable guidance, patience and support as an advisor over these years. I would also like to thank Dr. Lisa Robbins and Dr. Pamela Hallock Muller for agreeing to be on my committee and for their excellent feedback. I thank the members of the Byrne lab, past and present, for their contributions to my growth as a scientist; Katie Douglas and Bo Yang for helping me get acclimated to the lab my first year, Dr. Sherwood Liu and Dr. Kelly Quinn for providing guidance on lab techniques, Jon Sharp for being a great lab companion and helping tinker through spectrophotometer issues. I am thankful to Kira Barrera for her collaboration on the photometer project and Dr. Tonya Clayton for her insightful comments and edits to my manuscript.

My friends from the College of Marine Science, especially Kate Dubickas, have been such a great support and have made my time at CMS a fun and memorable experience. Special thanks to my parents, Janice and Richard Cuyler, and family members, Laurna and Mike Sheehan and Amy Marble, for always supporting and believing in me, I would not be where I am without you.

This research has been funded by the Von Rosenstiel Fellowship, the Gulf Oceanographic Charitable Trust Endowed Fellowship in Marine Science and the U.S. Geological Survey.

Table of Contents

List of Tables

List of Figures

Abstract

This work describes efforts to improve methodologies and instrumentation for investigation of the marine CO_2 system. In the first section of my thesis, a method was developed that provides simple, calibration-free measurements of seawater carbonate saturation states (Ω_{spec}) based solely on the use of a laboratory spectrophotometer. Measurements of pH are made in paired optical cells, one with and one without added nitric acid. The amount of added nitric acid is determined through the direct proportionality between nitrate concentration and UV absorbance. After an initial calibration, the method is calibration-free and requires no volumetric or gravimetric analyses thereafter. Saturation state measurements can be obtained in twelve minutes and attain Global Ocean Acidification Observing Network accuracy goals over a wide range of conditions. This simple one-step measurement protocol is ideal for monitoring ocean acidification conditions in coastal areas, fish hatcheries and shellfish farms.

The second section of my thesis outlines the development of a next-generation handheld photometer for field measurements of seawater pH. The hand-held instrument is simple to use, inexpensive, and has a pH measurement accuracy of ±0.01. Each photometer is calibrated by relating pH-indicator absorbance ratios (R_B) obtained with the broadband photometer to indicator absorbance ratios ($R_{N)}$ obtained with a high quality, narrowband scanning spectrophotometer. The R_B vs R_N relationship for each photometer is entered into the instrument's software, providing discrete, real-time pH observations from measurements of R_B, salinity and temperature. Measurement accuracy is assessed through comparisons of photometer pH with pH observations obtained using standard measurement procedures and high-quality

spectrophotometers. The targeted user-groups for these instruments include middle and high school students, citizen scientists, and resource managers

Introduction

Anthropogenic Impacts on the Marine CO_2 System

Since the industrial revolution, carbon dioxide emissions from fossil-fuel burning, deforestation, cement production, and gas flaring have increased the global atmospheric carbon dioxide concentration from approximately 280ppm, to present day levels of 408.8ppm [1]. That increase in CO_2 has been buffered by ocean uptake, which constitutes approximately 26% of cumulative anthropogenic CO_2 emissions [2]. Without this ocean sink, atmospheric CO_2 concentrations would be approximately 55 ppm higher than present day values [3]. However, absorption of CO_2 into the ocean has caused the mean surface ocean pH to decrease by 0.1 compared to preindustrial levels and is projected to decrease by another 0.3–0.4 units by year 2100 [4–6]. Great efforts have been made to investigate ocean acidification (OA) and to determine future impacts on marine ecosystems.

Ocean acidification has also led to reductions in carbonate saturation states worldwide. Carbonate saturation states control the calcification rates of many species of calcifying organisms, including corals, coccolithophorids, foraminifera, pteropods and bivalves, and research has linked reduced saturation states to reductions in calcification and productivity in these species [7–14]. High latitude regions are especially vulnerable to reductions in saturation states due to their higher capacity for CO_2 absorption and ocean mixing patterns [6,15]. Future projections of ocean acidification indicate that, in the absence of large reductions in fossil-fuel emissions, the entire Arctic Ocean and parts of the Southern Ocean will be undersaturated with respect to aragonite by 2050, and other regions that are not completely undersaturated will

experience substantial shoaling of their saturation horizons [16]. These changes profoundly affect calcifying plankton and benthic organisms that make up the base of the food web in those regions [16].

In coastal areas, complex biogeochemical processes that occur along with anthropogenically driven processes (i.e., hypoxia, nutrient loading), make investigating the effects of OA in these regions more complicated. Current ocean acidification models, which are based on open ocean characteristics and circulation patterns and lack input from the coastal environment, require further contributions of coastal data before their predictions can be confidently applied to those ecosystems [17]. The extent and severity of OA impacts on coastal ecosystems likely will depend on local ecosystem drivers, such as vegetation types, degree of influence from run off and eutrophication, presence and intensity of upwelling, and types of marine fauna present [17–19]. Coastal areas are important economic zones that support large fisheries and shellfish industries. Therefore, accurate monitoring of saturation states within these regions is crucial to ensuring their future viability [20].

Measurements of CO_2 System Parameters

The aqueous CO_2 system is characterized by observations of five measurable parameters: pH, total alkalinity (TA), total dissolved inorganic carbon (DIC), CO_2 fugacity (fCO_2), and carbonate concentration ($[CO_3^{2-}]_T$). Using thermodynamic relationships, measurements of any two of the five parameters can be used to calculate all others, including calcite and aragonite saturation states [21]. Precise and accurate measurements of each of the five carbon system parameters can be obtained using different instrument protocols.

pH

Ocean pH is measured either potentiometrically or spectrophotometrically. Potentiometric measurements are obtained using glass pH electrodes that have been calibrated with a tris buffer prepared in synthetic seawater [22]. Spectrophotometric pH measurements are obtained through an addition of a sulfonephthalein indicator dye [H_2I] to a seawater sample. Absorbance measurements are taken at the broad absorbance maxima of the acidic HI^- and basic I^{2-} forms of an indicator dye to obtain an absorbance ratio (R) which is subsequently used to calculate pH [23–26]. Meta-cresol purple (range: 7.2<pH<8.2) is the most common indicator used for seawater pH measurements [26] while cresol red [27] (range: 6.8<pH<7.8) and thymol blue [28] (range; 7.9<pH<8.9) are applicable at lower and higher pH ranges.

Recent improvements to seawater pH measurements have been implemented using Ion Selective Field Effect Transistor (ISFET) based sensors [29–31]. ISFET pH sensors experience less drift and noise than glass electrodes and, in some circumstances, have a faster response time than in situ spectrophotometric techniques [31]. Extensive testing of ISFET sensors indicate that their fast response time, high pressure tolerance, and measurement stability (better than 0.005 over weeks to months) make them appropriate for deployments on moorings, gliders, ROV's and CTD systems [30,31].

Total Dissolved Inorganic Carbon

To measure total dissolved inorganic carbon, a seawater sample is acidified with sufficient strong acid so that all forms of DIC (i.e., CO_2^*, HCO_3, and CO_3) are converted to CO_2 gas. The CO_2 is then transferred to a coulometer via inert nitrogen gas where it is titrated coulometrically to quantify DIC [21]. Alternatively, DIC can be measured using a CO_2 permeable membrane, such as a liquid core waveguide, that allows acidified seawater samples to

equilibrate with an internal reference solution with respect to pCO_2 [32]. The known alkalinity and measured equilibrium pH of the reference solution allows calculation of the total dissolved inorganic carbon in the acidified seawater.

Total Alkalinity

Total alkalinity can be measured by single step [33] or stepwise [34–36] additions of acid to a seawater sample. Subsequently, excess acid is measured by either potentiometric or spectrophotometric techniques, and algorithms can be used to determine the equivalence point on a titration curve. Potentiometric methods require frequent, precise calibrations of pH electrodes [36]. In spectrophotometric TA analysis, the final pH is measured with an indicator dye after a single step acid addition. Such procedures can improve precision, decrease measurement time, and obviate the need for frequent calibrations [37].

CO_2 Fugacity

CO2 fugacity can be measured using autonomous underway CO_2 fugacity analyzers. A continuous stream of seawater is taken up to equilibrate with a fixed volume of air contained within the system [21]. The CO_2 equilibrated air is then measured by infrared (IR) or gas chromatography. The system is calibrated with well-characterized CO_2 gas standards.

Carbonate Ion Concentrations

$[CO_3^{2-}]_T$ is the most recent addition to the group of measurable CO_2 system parameters. Seawater carbonate ion concentrations are measured via spectrophotometry. After addition of lead perchlorate ($PbClO_4$) to a seawater sample, absorbance measurements of UV spectra attributable to $PbCO_3$ and $PbCl_n$ complexes are used to quantify $[CO_3^{2-}]_T$ [38]. After initial calibrations in the laboratory, this method requires no subsequent calibrations.

Carbonate Saturation States

Carbonate saturation states are generally obtained from coupled measurements of two of the five carbon system parameters. Each measured parameter requires a different experimental set-up using a unique instrument, and substantial operator expertise to ensure measurement accuracy. As such, conventional carbonate saturation state measurements are substantially time consuming and expensive relative to measurements of a single CO_2 system parameter.

In response to increasing urgency to understand OA impacts on dynamic and vulnerable coastal zones, further development of simple and convenient methods to measure saturation states are highly desirable. The following thesis chapter addresses this need for improved measurements using a novel protocol to obtain carbonate saturation states solely via spectrophotometry. This measurement technique emphasizes simplicity and convenience at levels of precision and accuracy that are consistent with the high spatial and temporal variability of coastal zones.

Calibration-free Spectrophotometric Measurements of Carbonate Saturation States in Seawater

Abstract

A simple, calibration-free protocol was developed to measure seawater carbonate saturation state (Ω_{spec}) spectrophotometrically. Saturation states are typically derived from the separate measurement of two other carbon system parameters, with each parameter requiring unique instrumentation and often complex measurement protocols. The new method is a one-step protocol, with the only required equipment being a thermostatted laboratory spectrophotometer. For each seawater sample, spectrophotometric measurements of pH (visible absorbance) are made in paired optical cells, one with and one without added nitric acid. The amount of added acid is determined through the direct proportionality between nitrate concentration and ultraviolet (UV) absorbance. These paired absorbance measurements yield Ω_{spec} (and other carbonate system parameters), with each sample requiring about 12 minutes processing time. Initially, an instrument-specific nitrate molar absorptivity coefficient must be determined (due to small but significant discrepancies in instrumental wavelength calibrations), but thereafter, no further calibration is needed. In this work, the 1σ precision of replicate measurements of aragonite saturation state was 0.020, and the average difference between Ω_{spec} and Ω calculated conventionally from measured total alkalinity and pH (Ω_{calc}) was −0.11% ± 0.96% (a level of accuracy comparable to that obtained from spectrophotometric measurements of carbonate ion concentration). Over the entire range of experimental conditions, $0.97 < \Omega < 3.17$ ($n = 125$), all measurements attained the Global Ocean Acidification Observing Network's "weather level"

goal for accuracy and 90% attained the more stringent "climate level" goal. When Ω_{spec} was calculated from averages of duplicate samples (n = 56), the precision improved to 0.014 and the average difference between Ω_{spec} and Ω_{calc} improved to −0.11% ± 0.73%. Additionally, 97% of the duplicate-based Ω_{spec} measurements attained the "climate level" accuracy goal. These results indicate that the simple measurement protocol developed in this work should be widely applicable for monitoring fundamental seawater changes associated with ocean acidification.

Introduction

To date, the ocean has absorbed about 30% of the anthropogenic carbon dioxide (CO_2) emitted since the industrial revolution [2,39], thereby reducing pH and carbonate saturation states (Ω) throughout the surface ocean—i.e., ocean acidification (OA) [6,40–42]. Research into the impacts of ocean acidification has shown that lower saturation states cause calcification rates to decrease in many calcifying species [9–14]. Saturation state monitoring is crucial to understanding the diverse impacts of ocean acidification on marine ecosystems and coastal economies in the next century.

The seawater CO_2 system can be characterized by observations of five measurable carbon system parameters: pH, total alkalinity (A_T), total dissolved inorganic carbon (C_T), CO_2 fugacity (fCO_2), and total carbonate ion concentration ($[CO_3^{2-}]_T$). Models of carbon system thermodynamics allow for the calculation of all carbon system parameters (including calcite and aragonite saturation states) from any two of the measurable variables [21]. The parameter pair of C_T and A_T is frequently used for saturation state calculations. However, these measurements require two separate instrumental setups, and both protocols are somewhat complex and time-consuming. Additionally, attaining precise A_T measurements requires meticulous gravimetric or volumetric measurements of the acid added during analytical titrations (i.e., seawater:acid

mixing ratios) [37]; this requirement can be especially challenging for shipboard measurements. A simpler, faster, and more convenient method for determining carbonate saturation state would be beneficial for the widespread monitoring of ocean acidification.

Previously, tracer additions have been used to quantify titrant additions without the use of volumetric or gravimetric analysis [43]. For example, the seawater alkalinity measurements of Spaulding et al. (2014) [44] use a sulfonephthalein pH indicator dissolved in a hydrochloric acid titrant to precisely quantify tracer:acid concentration ratios and monitor acid delivery.

An alternative approach is to use the physical properties of the acid itself to monitor titrant additions. Nitric acid (HNO_3), for example, absorbs light in the ultraviolet (UV) range. Therefore, the direct (Beers Law) relationship between nitrate concentration and nitrate UV absorbance can be used to monitor additions of nitric acid without the need for meticulous preparation and characterization of indicator:acid mixtures.

In this work, we demonstrate that aragonite saturation state can be precisely and accurately determined by measuring visible and UV absorbances in paired spectrophotometric cells, one with and one without added nitric acid. From these two sets of absorbance measurements, the entire suite of carbonate system parameters can be obtained.

Theory

The relationship between total alkalinity (A_T) and total dissolved inorganic carbon in a seawater sample is given as [45]

$$A_T = C_T \left(\frac{2 \cdot K_1' \cdot K_2' + K_1' \cdot [H^+]}{K_1' \cdot K_2' + K_1' \cdot [H^+] + ([H^+])^2} \right) + \frac{B_T \cdot K_B'}{K_B' + [H^+]} + \frac{K_W'}{[H^+]} - [H^+] \quad (1)$$

where K_1', K_2', K_B', and K_W' are the dissociation constants of carbonic acid, bicarbonate, boric acid, and water in seawater, and B_T is the total boron concentration; these variables are expressed in units of moles kg^{-1}. (Additional terms for nutrients and organic alkalinity are not explicitly

shown here.) The term $[H^+]$ represents total hydrogen ion concentration, which is obtained from measurements of seawater pH ($pH = -\log[H^+]$).

Our experimental protocol relies on the use of paired, initially identical seawater subsamples and a one-step titration using nitric acid. Initial conditions of the seawater (subsample 1) are indicated by subscript $_1$, and conditions after a one-step HNO_3 addition (subsample 2) are indicated by subscript $_2$. When the HNO_3 is added, the initial A_{T1} of the seawater is decreased by an amount equal to the change in NO_3^- concentration (ΔNO_3^-); C_T and B_T are unchanged. Conditions before and after acidification are related as follows:

$$A_{T2} = \theta \cdot A_{T1} - \Delta NO_3^- = \theta \cdot C_T \left(\frac{2 \cdot K_1' \cdot K_2' + K_1' \cdot [H^+]_2}{K_1' \cdot K_2' + K_1' \cdot [H^+]_2 + ([H^+]_2)^2} \right) + \theta \cdot \frac{B_T \cdot K_B'}{K_B' + [H^+]_2} + \frac{K_W'}{[H^+]_2} - [H^+]_2 \quad (2)$$

where the dilution factor θ is given by

$$\theta = \frac{V_{sw}}{V_{sw} + V_{HNO3}} \quad (3)$$

V_{SW} is the initial volume of seawater, and V_{HNO3} is the volume of added nitric acid. This θ term accounts for the minor dilution of A_{T1}, C_T, and B_T caused by the acid addition.

The ΔNO_3^- term in Eq. (2) can be obtained from spectrophotometric measurements of absorbance A at wavelength λ, in combination with Beer's Law: $_\lambda A = C\, l\, {}_\lambda\varepsilon$, where C is the concentration of the absorbing analyte, l is the spectrophotometric cell path length, and $_\lambda\varepsilon$ is the molar absorptivity coefficient of the absorbing constituent. The resulting equation is

$$\Delta NO_3^- = \frac{{}_{235}A_{NO3}}{l \cdot {}_{235}\varepsilon_{NO3} \cdot \rho_{sw}} \quad (4)$$

where $_{235}A_{NO3}$ is the nitrate absorbance at 235 nm, $_{235}\varepsilon_{NO3}$ is the molar absorptivity coefficient of nitrate at 235 nm and 25 °C, and ρ_{sw} is the density of the seawater (a function of salinity S and temperature T [46]). Routine baseline corrections applied to the absorbance measurements subtract out the effects of any nitrate initially in the seawater sample. The ρ_{sw} term is required to

yield ΔNO_3^- in the desired concentration units (mole kg^{-1}).

With spectrophotometric measurements of pH_1 and pH_2 [21,26], Eqs. (1) and (2) can be used to calculate C_T and A_{T1} of the original seawater sample. For convenience, the equations are first simplified by defining the following parameters:

$$f_C = \frac{2 \cdot K_1' \cdot K_2' + K_1' \cdot [H^+]}{K_1' \cdot K_2' + K_1' \cdot [H^+] + ([H^+])^2} \quad (5)$$

$$f_B = \frac{B_T \cdot K_B'}{K_B' + [H^+]} \quad (6)$$

$$f_W = \frac{K_W'}{[H^+]} - [H^+] \quad (7)$$

where f_C is related to carbonate alkalinity, f_B is borate alkalinity, and f_W is hydroxide alkalinity minus the hydrogen ion concentration. The dissociation constants within these functions depend on *S*, *T*, and hydrostatic pressure *P*.

Eq. (1), which applies to the unacidified seawater, can now be written as

$$A_{T1} = C_T \cdot f_{C1} + f_{B1} + f_{W1} \quad (8)$$

Eq. (2), which applies to the acidified seawater, can be written as

$$A_{T2} = \theta A_{T1} - \Delta NO_3^- = \theta C_T \cdot f_{C2} + \theta f_{B2} + f_{W2} \quad (9)$$

To obtain the seawater C_T (which is not directly changed by the addition of nitric acid), Eq. (9) can be rearranged and written in a form similar to Eq. (8):

$$A_{T1} = C_T \cdot f_{C2} + f_{B2} + \theta^{-1} \Delta NO_3^- + \theta^{-1} f_{W2} \quad (10)$$

By subtracting Eq. (8) from Eq. (10), A_{T1} is eliminated and C_T is expressed directly in terms of f_C, f_B, f_W, and θ:

$$C_T(f_{C1} - f_{C2}) = \theta^{-1} \Delta NO_3^- + f_{B2} - f_{B1} + \theta^{-1} f_{W2} - f_{W1} \quad (11)$$

After rearrangement, C_T is given explicitly as

$$C_T = \frac{\theta^{-1}\Delta NO_3^- + f_{B2} - f_{B1} + \theta^{-1} f_{W2} - f_{W1}}{f_{C1} - f_{C2}} \quad (12)$$

The total alkalinity of the original seawater solution (A_{T1}) can then be calculated using this value of C_T (Eq. 12) in Eq. (8).

The carbonate ion concentration ($[CO_3^{2-}]_T$) can be calculated from C_T (Eq. 12), A_{T1} (Eq. 8), and the measured *S* and in situ *T* of the seawater sample.

Finally, carbonate saturation state is calculated from

$$\Omega = \frac{[CO_3^{2-}]_T \cdot [Ca^{2+}]_T}{K'_{sp}} \quad (13)$$

where $[Ca^{2+}]_T$ is the total calcium ion concentration, and K'_{sp} is the solubility product of the calcium carbonate polymorph of interest (e.g., calcite or aragonite). The calcium term is calculated from the direct proportionality between calcium and salinity: $[Ca^{2+}] = 0.0102821 * S/35$ [47]. In this work, we focus on aragonite saturation states because aragonite is the more soluble of the two major calcium carbonate polymorphs.

Materials and Methods

Equipment, Sample Solutions, and Reagents

Spectrophotometric measurements of ${}_{235}\varepsilon_{NO3}$ were made with a high-quality, dual-beam scanning spectrophotometer (Agilent Cary 400 Bio UV-VIS). Each time the Agilent Cary 400 is powered on, it performs an internal wavelength accuracy calibration by detecting the sharp emission lines of a deuterium lamp; the wavelength accuracy specification is ±0.08 nm [48]. This large benchtop spectrophotometer was fitted with a custom-made 10 cm pathlength open-top quartz cell (Precision Cells, Inc.).

Spectrophotometric measurements of apparent nitrate molar absorptivity coefficients and Ω were made with less expensive, more portable diode array spectrophotometers suitable for

fieldwork (Agilent model 8453). This instrument has a wavelength accuracy of ±0.5 nm [49]. Two-port 10 cm cylindrical quartz cells (Starna Cells, Inc.) were used for all measurements. The four portable Agilent instruments used in this work are identified as spec1, spec2 (a and b), spec3 (a and b), and spec4. An *a* or *b* suffix (e.g., spec2a, spec2b) indicates wavelength recalibration: *a* indicates the state of the instrument before recalibration, and *b* indicates the state after recalibration.

For temperature control, all spectrophotometers were connected to a recirculating water bath (Lauda model E100) via insulated tubing, and a digital thermometer (ERTCO EUTECHNICS model 4400) was used to monitor solution temperature. A Guildline Portasal salinometer (model 8410) was used to measure seawater salinity, and Gilmont micrometer syringes (model GS-1200) were used to deliver liquid reagents.

Natural seawater collected from offshore surface waters of the Gulf of Mexico was used for all analyses. Nucleopore membrane filters (0.4 µm, Lot 81D5A4) were used to filter seawater for the $_{235}\varepsilon_{NO3}$ measurements performed on the Cary 400 spectrophotometer; all other analyses used unfiltered seawater. The seawater was stored in a 50 L Nalgene container for later use; this container was sealed to prevent evaporation. Total alkalinity (A_T) of the seawater was measured spectrophotometrically, following the procedure of Yao and Byrne [37]; an accuracy of better than ± 2 µmol kg^{-1} was confirmed using certified reference materials from the Scripps Institution of Oceanography. A_T was re-measured periodically to verify the absence of changes attributable to dehydration. To achieve a range of experimental conditions for this work (i.e., seawater saturation states and pH), samples were bubbled with CO_2 gas.

The spectrophotometric pH measurements were conducted using meta-cresol purple (mCP) indicator (Aldrich, Lot 7005HH) and cresol red (CR) indicator (Biosynth, Lot

220307/11), both purified by flash chromatography [50]. Nitric acid standardizations were conducted using unpurified phenol red (Acros Organics). Stock solutions of the indicators (10 mM) in sodium chloride solutions (0.7 M) were prepared using NaCl obtained from MP Biomedicals. Trace metal–grade nitric acid was obtained from Fischer Scientific, and sodium carbonate (99.95%, extra pure, anhydrous) was obtained from Acros Organics. Anaerobe-grade carbon dioxide was obtained from Air Products, and ultra-pure N_2 was obtained from Airgas.

The nitric acid was standardized by titration of sodium carbonate solutions, generally following the procedure outlined in Chapter 11 of Harris (2007) [51]. Procedural modifications included the use of phenol red indicator (instead of bromocresol green), as well as the use of streaming nitrogen gas (instead of boiling) to purge the solution of CO_2.

Carbonate System Calculations

All carbonate system calculations were conducted using the Microsoft Excel program CO2SYS [52]. The constants K_1 and K_2 were taken from Lueker et al. (2000) [53]; K_B was taken from Dickson (1990) [54]; K_W was taken from Millero (1995) [55]; K_{sp} was taken from Mucci (1983) [56]; the bisulfate dissociation constant (K_{HSO4}) was taken from Dickson (1990) [57]; and the dependence of B_T on salinity was taken from Uppström (1974) [58].

Determination of Dilution Factor

The dilution factor θ of Eq. (3) was determined as a function of ${}_{235}A_{NO3}$ (using spec1). Spectrophotometric cells were filled with seawater, and UV absorbances (235, 236, 237, 238, and 239 nm) were measured before and after additions of HNO_3 from a micrometer syringe. The resulting ΔNO_3^- range was $164.7 < \Delta NO_3^- < 553.0$ µM. The initial volumes of seawater contained within the cells (V_{SW}) were determined by gravimetric calibration with Milli-Q® water [21]. Volumes of added acid (V_{HNO3}) were obtained by weighing the syringe before and after

each addition. A value of θ was then calculated (Eq. (3)) for each nitrate concentration, and linear regression was used to characterize θ as a function of ${}_{235}A_{NO3}$.

Measurements of ${}_{\lambda}\varepsilon_{NO3}$

To determine the molar absorptivity of nitrate, the Cary 400 spectrophotometer was used to measure seawater absorbance at selected wavelengths over a range of nitrate concentrations. The wavelengths used were 235, 236, 237, 238, 239 (on the shoulder of the 225 nm nitrate absorbance peak) and 385 nm (a non-absorbing wavelength). These wavelengths were chosen to yield absorbance values appropriate for the range of experimental nitrate concentrations and the characteristics of the spectrophotometers and cell pathlengths being used. The absorbance measured at the non-absorbing wavelength, which was used to monitor and correct for potential baseline shifts, was maintained within ±0.002. The range of ΔNO_3^- was $335.0 \leq \Delta NO_3^- \leq 525.9$ μM.

For each of these analyses, approximately 100 mL of filtered seawater was transferred to the open-top quartz cell, which was then placed into the Cary 400 spectrophotometer. Baseline absorbance measurements were taken at the six UV wavelengths, and five increments of nitric acid (0.477 ± 0.001 M) were added to the seawater sample (approximately 70 μL for the first addition, with additions of 10 μL thereafter); absorbances were remeasured after each addition. The amounts of added HNO_3 were determined by weighing the delivering syringe before and after each acid addition. The resulting five nitrate concentrations were then used in Eq. 4 to yield an average ${}_{\lambda}\varepsilon_{NO3}$ value for each absorbing wavelength. Solutions were maintained at 25 °C ± 0.1 throughout all experiments.

Nitrate molar absorptivity values were similarly obtained using the portable Agilent spectrophotometers spec2, spec3, and spec4, and these instrument-specific values are hereafter

referred to as apparent molar absorptivities ($_{\lambda}\varepsilon^{*}_{NO3}$). Absorbance measurements were made at 1 nm intervals between 235 and 239 nm and at 385 nm. The nitric acid concentration was 300 ± 0.5 µM. Eq. 4 was used to calculate a $_{\lambda}\varepsilon^{*}_{NO3}$ value for each instrument.

Spectrophotometric Determination of Carbonate Saturation State

Each saturation state determination requires two spectrophotometric cells, each filled with a subsample of identical seawater. The first cell is used to measure the pH of the original seawater, and the second cell is used to measure the pH of the same seawater after the one-step addition of titrant (nitric acid). For these analyses, seawater was drawn directly from the 50 L storage container into the optical cells. Each cell was flushed with seawater for 20 seconds before being sealed with Teflon caps, then rinsed with tap water, dried with a paper towel, and placed in a custom-made cell warmer to thermally equilibrate to 25°C. In all analyses, cells were handled with a foam holder to minimize heat transfer. After thermal equilibration, the optical windows were wiped clean with a Kimwipe, and the cells were placed in the spectrophotometer for absorbance measurements.

For the first cell, the pH of the seawater sample (pH_1) was measured spectrophotometrically following the procedure of Clayton and Byrne (1993) [26], as summarized by standard operating procedure (SOP) 6b of Dickson et al. (2007) [21]. The indicator mCP [26,59] was used for samples with $pH_1 > 7.8$, and CR [27] was used for samples with $pH_1 < 7.8$. For mCP, absorbances were measured at 434, 578, and 730 nm; for CR, absorbances were measured at 433, 573, and 730 nm. The non-absorbing wavelength, 730 nm, was used to monitor and correct for baseline shifts. Two 10 µL additions of indicator were performed, and absorbance measurements were taken after each addition. This procedure provides corrections for the small pH perturbations created by indicator additions [26,27].

For the second (i.e., titrated) cell, UV absorbance measurements were first made to determine the amount of added acid, and then visible absorbance measurements were made to determine the final pH (pH_2) of the sample. First, a background absorbance measurement was taken at 235 nm and 385 nm. The cell was then acidified with a volume of HNO_3 sufficient to significantly depress the pH relative to pH_1, typically to ~7.2 but occasionally (i.e., when $pH_1 <$ 7.8) to ~6.8. The amount of required HNO_3 ranged from 14–19 µL and was dependent on the value of pH_1. After acidification, the cell was manually mixed and then returned to the spectrophotometer's thermostated cell compartment. Absorbance measurements for the determination of ΔNO_3^- were taken at 235 nm and 385 nm, with ${}_{385}A$ being used for baseline corrections. Finally, pH_2 was measured using the same visible-absorbance protocol as was used for the first cell.

These paired sets of absorbance measurements were used to derive carbonate system parameters as outlined in the theory section (see Appendix B for example calculation). Values of $[H^+]_1$ and $[H^+]_2$ were calculated from pH_1 and pH_2. Values of f_C, f_B, and f_W can be calculated directly from Eqs. (5), (6), and (7), but for convenience we used the program CO2SYS (which includes code to characterize the multiple dissociation constants as a function of *S*, *T*, and *P*). To obtain f_B and f_W, we rely on the fact that these terms are a function of pH and are independent of C_T. The cell pH and an arbitrary C_T value ($C_{T(A)}$) were supplied to CO2SYS as input parameters, along with the appropriate *S*, *T*, and *P* values. The resulting CO2SYS output included borate alkalinity and hydroxide alkalinity, which were then used in Eqs. (6) and (7) to obtain f_B and f_W. To obtain f_C, CO2SYS was used to model a change in the inorganic carbon content of a hypothetical seawater sample at constant pH. Because f_B and f_W are constant at constant pH, any resulting change in A_T can be attributed solely to f_C (Eq. (8)). For each cell pH (i.e., pH_1 and

pH_2), two different, arbitrary C_T values (an initial value $C_{T(A)}$ and a final value $C_{T(B)}$) were specified as input parameters. From the resulting A_T values ($A_{T(A)}$ and $A_{T(B)}$), a value of f_C was calculated as the ratio of the change in A_T to the change in C_T at the specified pH:

$$f_{CX} = \frac{A_{T(B)} - A_{T(A)}}{C_{T(B)} - C_{T(A)}} \quad (14)$$

where *X* refers to pH_1 or pH_2.

With these values in hand, carbonate saturation states can be determined. Values of C_T (obtained from Eq (12)) and A_{T1} (obtained from Eq (8)) were input into CO2SYS (along with *S*, *T*, and *P*) to calculate aragonite saturation state (Ω_{spec}). The accuracy of the Ω_{spec} measurements, $\Delta\Omega_{spec}$, was determined by comparing Ω_{spec} with conventionally calculated aragonite saturation states (Ω_{calc}) obtained using the independently measured values of A_{T1} and pH_1.

Results

Dilution Factor as a Function of $_{235}A_{NO3}$

The relationship between dilution factor θ (Eq. (3)) and UV absorbance at 235 nm (a proxy for the concentration of added nitrate in a sample) is given by:

$$\theta = 1 - 0.000776 * {}_{235}A_{NO3} \quad (15)$$

The linear regression used to obtain this relationship is shown in Fig. 1. This equation is based on additions of 0.477 M HNO_3. For different concentrations of nitric acid, the slope will change by a factor of $0.477[HNO_3]^{-1}$. It is important to note that θ is a small correction factor in Eq. (12). In the present study, dilution corrections changed A_{T1} and C_T by 1–2 µmol kg^{-1} and changed Ω_{spec} by ~0.005. In each case, the dilution correction is far smaller than the measurement imprecision.

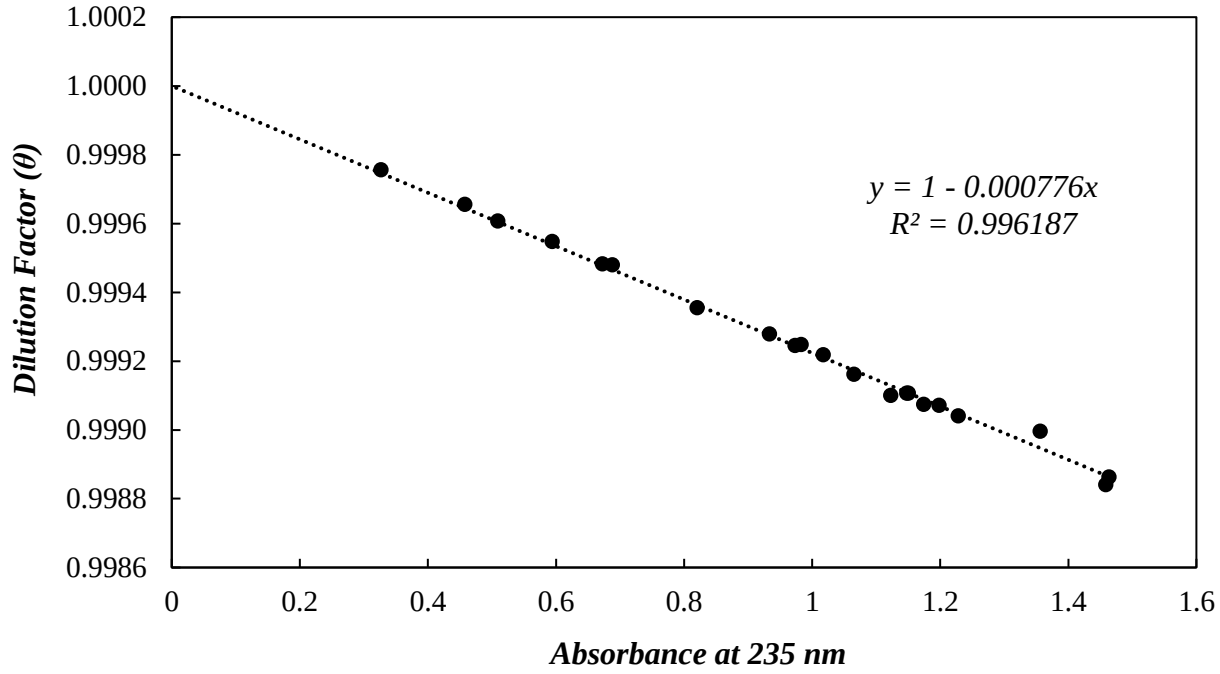

Figure 1: Relationship between the Eq. (3) dilution factor θ and UV absorbance measured at 235 nm, using 10 cm cylindrical cells. This equation is appropriate for a titrant concentration of 0.477 M HNO_3.

Nitrate Molar Absorptivity Coefficients

Nitrate molar absorptivity coefficients ($_{\lambda}\varepsilon_{NO3}$) measured on the Cary 400 Bio spectrophotometer at 1 nm intervals over the wavelength range 235–239 nm are presented in Table 1. The standard errors (1σ) of all $_{\lambda}\varepsilon_{NO3}$ values are <0.2%. The relationship between ΔNO_3^- and $_{235}A_{NO3}$ follows Beers Law, as expected. We consider these high-quality measurements to represent actual nitrate molar absorptivity coefficients.

Table 1: Nitrate molar absorptivity coefficients at selected wavelengths ($_{\lambda}\varepsilon_{NO3}$ ± standard error) measured with an Agilent Cary 400 Bio spectrophotometer at 25 °C.

Wavelength (nm)	$_{\lambda}\varepsilon_{NO3}$ **± SE (cm^2 mole^{-1})[a]**
235	276.6 ± 0.59
236	223.7 ± 0.40
237	180.4 ± 0.26
238	149.6 ± 0.14
239	118.9 ± 0.11

[a] Average of 5 absorbance measurements at each wavelength

Apparent nitrate molar absorptivity coefficients measured on the portable Agilent spectrophotometers spec2, spec3, and spec4 at 235 nm are given in Table 2. All measurements were conducted at the same nitrate concentration, but the difference among the observed $_{235}A_{NO3}$ values obtained with different instruments was as large as 0.035. Because these coefficients are instrument-specific, we refer to them as apparent molar absorptivity coefficients, $_{235}\varepsilon^{*}_{NO3}$. For each spectrophotometer, these different values were tracked and used for all subsequent calculations. (A value of $_{235}\varepsilon^{*}_{NO3}$was not determined for spec1; all spec1-based calculations used the $_{235}\varepsilon_{NO3}$ value reported in Table 1.) The differences between the Table 1 (actual) and Table 2 (apparent) molar absorptivities are due to sub-nanometer offsets in the wavelength calibrations of the Agilent instruments. When determining nitric acid concentrations via Eq. 4, $_{235}\varepsilon^{*}_{NO3}$ values specific to each instrument must be used.

Table 2: Apparent nitrate molar absorptivity coefficients ($_{235}\varepsilon^{*}_{NO3}$) measured at 235 nm on portable Agilent spectrophotometers.

Spectrophotometer[a]	**$_{235}\varepsilon^{*}_{NO3}$ ± SE (cm^2 mole^{-1})[b]**
spec2a	277.4 ± 0.05
spec2b	288.0 ± 0.04
spec3a	285.5 ± 0.04
spec3b	274.0 ± 0.03
spec4	281.2 ± 0.05

[a] The *a* and *b* suffixes indicate determinations made before (*a*) and after (*b*) spectrophotometer recalibration.

[b] Values of $_{235}\varepsilon^{*}_{NO3}$ were calculated as the average value of four absorbance measurements.

Accuracy and Precision of Ω_{spec} *Measurements*

In our assessments of accuracy, any difference between Ω_{spec} and Ω_{calc} (where $\Delta\Omega_{spec} = \Omega_{spec} - \Omega_{calc}$) is considered to be a measurement error attributable to Ω_{spec}. Values of $\Delta\Omega_{spec}$ greater than 3 standard deviations from the mean were considered to be outliers and were removed (3.3% of all Ω_{spec} measurements).

Figure 2 and Table 3 show the percent errors for aragonite saturation state measured with the four portable Agilent spectrophotometers; Table 3 also shows the range of experimental conditions. For spec1 (n = 87), the errors center about zero (indicating that the wavelength calibrations of the Cary 400 and spec1 were fortuitously close); the mean and standard deviation

of the percent errors are 0.05% ± 1.73%. For spec2, spec3, and spec4 (combined n = 125), the percent errors uniformly scatter about zero; the mean and standard deviation are −0.11% ± 0.96%. In Fig. 2, results for low-Ω seawater (Ω_{calc} < 1.18) are shown in red, and those for high-Ω seawater (Ω_{calc} > 2.37) are shown in black; no samples fell into the intermediate Ω range. The corresponding ranges of pH_1 were 7.42–7.48 (low-Ω samples) and 7.84–8.03 (high- Ω samples).

The measurements performed on spec1 exhibited significantly worse accuracy than measurements performed on the other three instruments (Fig. 2) due to a faulty (unstable) cell holder. Therefore, the discussions that follow refer exclusively to the measurements performed on spec2, spec3, and spec4.

Table 3: Accuracy of Ω_{spec} measurements obtained on the four portable Agilent spectrophotometers.

Spectrophotometer	***n*[a]**	**Ω_{calc} range**	**Ω_{spec} range**	**$\Delta\Omega_{spec}$[b] (average ± 1σ)**	**$\Delta\Omega_{spec}$ % error (average ± 1σ)**
spec1	87	2.50 – 3.73	2.46 – 3.77	0.00 ± 0.05	0.05% ± 1.73%
spec2 high-Ω	59	2.37 – 3.17	2.35 – 3.20	−0.01 ± 0.02	−0.18% ± 0.83%
spec2 low-Ω	26	0.97 – 1.18	0.98 – 1.20	0.01 ± 0.01	0.56% ± 0.95%
spec3	20	3.03 – 3.17	3.01 – 3.11	−0.01 ± 0.03	−0.22% ± 0.92%
spec4	20	3.00 – 3.14	2.98 – 3.11	−0.02 ± 0.03	−0.65% ± 0.96%

[a] n = number of measurements

[b] $\Delta\Omega_{spec} = \Omega_{spec} - \Omega_{calc}$

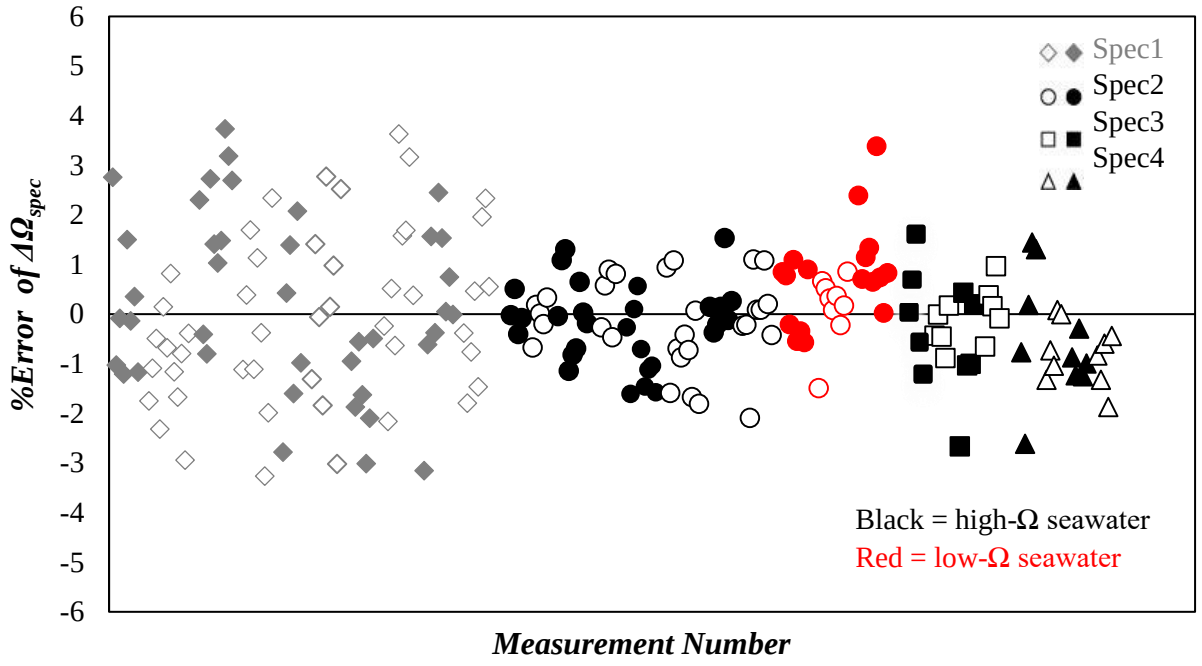

Figure 2: Percent error in aragonite saturation state measurements from the four portable Agilent spectrophotometers ($\Delta\Omega_{spec} = \Omega_{spec} - \Omega_{calc}$). The left-to-right alternating series of filled and empty symbols depict the different batches of measurements (29 batches, 212 total measurements). Values for high-Ω seawater ($\Omega_{spec} > 2.37$) are shown in black, and values for low-Ω seawater ($\Omega_{spec} < 1.18$) are shown in red. The data from spec1 (all high-Ω) are shown in gray because the data were somewhat compromised by a faulty cell holder and perhaps also operator inexperience.

Overall, 72% of the measured Ω_{spec} values were within 1% of the conventionally calculated saturation states, and 96% were within 2% of the calculated values. Estimates of Ω_{spec} precision are given as the combined standard deviation (1σ) of replicate measurements [60]. For the pool of measurements obtained using spec2, spec3, and spec4, the Ω_{spec} precision was 0.020. Relative standard uncertainty (RSU) values were also obtained from the mean (μ) and standard

deviation (σ) of batches of replicate measurements (RSU = $\sigma\ \mu^{-1}$ *100). Overall, 90% of the measurements had RSUs <1%, and all measurements had RSUs <2%.

Accuracy and Precision of $[CO_3^{2-}]_{Tspec}$ and fCO_{2spec} Measurements

For each seawater sample, carbonate ion concentration and CO_2 fugacity were also calculated from the spectrophotometrically determined values of C_T (Eq. (12)) and A_{T1} (Eq. 8)). Figure 3 shows the percent errors for $[CO_3^{2-}]_{Tspec}$ and fCO_{2spec}. For spec2, spec3, and spec4, the measurements included high carbonate concentrations ($[CO_3^{2-}]_{Tcalc} \geq 147.1$ µmol kg^{-1}, in the high-Ω samples) and low carbonate concentrations ($[CO_3^{2-}]_{Tcalc} \leq 75.6$ µmol kg^{-1}, in the low-Ω samples). Values of fCO_{2calc} ranged from 416 µatm (high-Ω samples) to 2073 µatm (low-Ω samples). Table 4 presents the average and standard deviation of the $[CO_3^{2-}]_{Tspec}$ and fCO_{2spec} residuals for each sample type.

Table 4 : Accuracy of $[CO_3^{2-}]_{Tspec}$ and fCO_{2spec} measurements (n = 125).

	$\Delta[CO_3^{2-}]_{Tspec}$ (average ± 1σ)	**ΔfCO_{2spec} (average ± 1σ)**
High-Ω seawater[a]		
$147.1 < [CO_3^{2-}]_{Tcalc} < 198.8$ µmol kg^{-1}	−0.5 ± 1.6 µmol kg^{-1}	−1.3 ± 4.3 µatm
$416 < fCO_{2calc} < 658$ µatm		
Low-Ω seawater[b]		
$61.2 < [CO_3^{2-}]_{Tcalc} < 75.6$ µmol kg^{-1}	0.4 ± 0.6 µmol kg^{-1}	11.1 ± 18.9 µatm
$1803 < fCO_{2calc} < 2073$ µatm		

[a] High-Ω seawater is defined as $\Omega_{calc} > 2.37$

[b] Low-Ω seawater is defined as $\Omega_{calc} < 1.18$

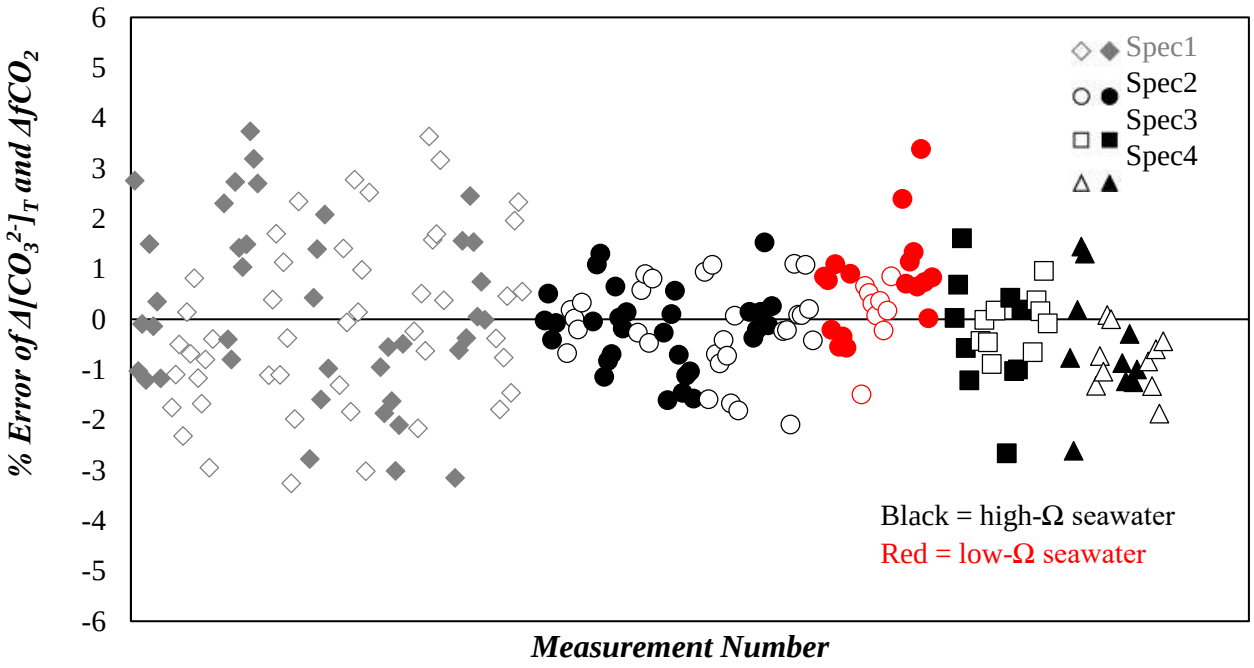

Figure 3: Percent errors in $[CO_3^{2-}]_{Tspec}$ and fCO_{2spec} determinations derived from absorbance measurements on the four portable spectrophotometers ($\Delta X_{spec} = X_{spec} - X_{calc}$). The left-to-right alternating series of filled and empty symbols depict the different batches of measurements (29 batches, 212 total measurements). Percent errors of $[CO_3^{2-}]_{Tspec}$ and fCO_{2spec} were nearly identical (within 0.06%), so the average value is shown for each sample. Samples of high-Ω seawater ($\Omega_{spec} > 2.37$) are shown in black, and low-Ω samples ($\Omega_{spec} < 1.18$) are shown in red. The data from spec1 (all high-Ω) are shown in gray because the data were somewhat compromised by a faulty cell holder and perhaps also operator inexperience.

Figure 3 shows that, like the Ω_{spec} measurements, 72% of the $[CO_3^{2-}]_{Tspec}$ and fCO_{2spec} measurements were within 1% of the values calculated from the pH_1–A_T measurements, and 96% were within 2% of the calculated values. RSU values for the $[CO_3^{2-}]_{Tspec}$ measurements were also similar to the RSUs obtained for Ω_{spec}: 90% of the $[CO_3^{2-}]_{Tspec}$ measurements had

RSUs <1%, and all had RSUs <2%. For fCO_{2spec}, 26% of the measurements had RSUs <1%, and 54% had RSUs <2%.

Gains in Accuracy and Precision Through Duplicate Measurements

The results in Figs. 2 and 3 and Tables 3 and 4 are based on single samples. The extent to which improvements in precision and accuracy might be realized by using averages obtained from duplicate samples was also assessed. Specifically, values of $\Omega_{spec,}$ $[CO_3^{2-}]_{Tspec}$, and fCO_{2spec} were calculated from average values of C_T (Eq. (12)) and A_{T1} (Eq. (8)) obtained from two measurements of identical seawater samples.

For Ω_{spec}, the combined, duplicate-based (spec2, spec3, and spec4) mean and standard deviation of the percent errors were −0.11% ± 0.73% (compared to −0.11% ± 0.96% for the single-sample errors); the 95% confidence interval (CI) was ±1.3% (down from ±2.0% for the single-sample measurements). The precision [33] of Ω_{spec} improved from 0.020 to 0.014. The percentage of measurements with RSUs <1% increased from 90% (single samples) to 97% (duplicate samples), and all duplicate-based Ω_{spec} measurements had RSUs <1.4%.

For $[CO_3^{2-}]_{Tspec}$ and fCO_{2spec}, the duplicate-based mean and standard deviation of the percent errors were −0.11% ± 0.73% (compared to −11% ± 0.96% for the single-sample errors); the 95% CI for the duplicate-based measurements was ±1.3% (down from ±2.0% for the single-sample measurements). The RSUs for the duplicate-based $[CO_3^{2-}]_{Tspec}$ measurements were similar to those for Ω_{spec}: the percentage of measurements with RSUs <1% increased from 90% (single samples) to 97% (duplicate samples), and all duplicate-based $[CO_3^{2-}]_{Tspec}$ measurements had RSUs <1.4%. For the duplicate-based fCO_{2spec} measurements, the percentage of measurements with RSUs <1% increased from 26% (single samples) to 78%, and 97% had RSUs <2% (up from 54% for the single-sample measurements).

Discussion

This work documents the accuracy and precision that can be achieved for calcium carbonate saturation state determinations obtained solely via spectrophotometry. Sulfonephthalein indicator absorbances at visible wavelengths are used to precisely quantify the pH of natural and acidified seawater samples. After a single-step titration with nitric acid, the direct (Beers Law) relationship between nitrate concentration and UV absorbance is used to quantify the seawater:acid mixing ratio. Using this protocol, the need for gravimetric or volumetric measurements to quantify amounts of added acid is eliminated and the only instrumentation required is a standard spectrophotometer. The measurements are simple and convenient, and each measurement is obtained in about 12 minutes. The utilization of nitric acid for titrations increases the simplicity and speed of the saturation state determinations without causing substantial loss of precision and accuracy.

The Global Ocean Acidification Observing Network (GOA-ON) has formulated accuracy goals [61] that serve as useful metrics for assessing the utility of seawater carbonate system measurements, based on the relative standard uncertainty of the measurements. GOA-ON data that achieve the "weather level" accuracy goals can be used to assess short-term spatial and temporal patterns and to help interpret ecosystem responses to localized OA dynamics ; data that achieve the more demanding "climate level" goals can be used to assess long-term anthropogenically driven changes in carbon chemistry [61].

For our single-sample Ω_{spec} and $[CO_3^{2-}]_{Tspec}$ measurements, 100% of the measurements exhibited RSUs <2%, which is well within the GOA-ON "weather level" accuracy goals of RSU <10% [61]. Moreover, 90% of these measurements achieved the "climate level" accuracy goals of RSU <1% [61]. The 10% of the measurements that did not achieve the climate goal were

made in low-Ω waters (where $\Omega_{calc} < 1.18$ and $[CO_3^{2-}]_T < 75.6$ µmol kg^{-1}). For our fCO_{2spec} samples, 92% of the measurements achieved the "weather level" accuracy goal of RSU <2.5% [61]. Additionally, 27% of these measurements achieved the "climate level" goal of RSU <1% [61].

Performance of this method can be improved by using average C_T and A_{T1} values (Eqs. (12) and (8)) obtained from measurements of duplicate samples. For Ω_{spec} and $[CO_3^{2-}]_{Tspec}$, this additional effort would not be justified if "weather level" accuracy is the aim because this goal is already achieved 100% of the time through single-sample measurements. However, if long-term "climate level" monitoring is the goal, then the significant gains achieved through duplicate measurements becomes important. Using the duplicate-sample approach, 97% of our Ω_{spec} and $[CO_3^{2-}]_{Tspec}$ measurements achieved the "climate level" goals of accuracy (up from 90% for the single-sample approach). In addition, the percentage of fCO_{2spec} measurements that achieved the "weather level" goal increased to 96% (previously 92%) and the percentage that reached the "climate level" goal increased to 73% (previously 26%). Running duplicate samples doubles the measurement time required to 24 minutes per sample, but the increases in precision and accuracy may be beneficial and even essential in some circumstances.

Figure 2 illustrates how the accuracy of the Ω_{spec} method may be improved through operator care and experience. The scatter of $\Delta\Omega_{spec}$ values associated with spec1 were substantially larger than the scatter associated with spec2, spec3, and spec4. The source of the disparity was, in part, a somewhat uneven spec1 cell compartment that made it difficult to maintain congruent cell orientation between the baseline and absrobance measurements. This led to comparatively large baseline shifts (>0.006) for the absorbance measurements performed on spec1 compared to the measurements performed on spec2, spec3, and spec4 which were nearly

all <0.003. Another contributing factor could be that the spec1 data were from the earliest experiments, and operator skill (i.e., sample handling) likely improved through time. The smaller standard deviations of the spec2, spec3, and spec4 data likely provide a better representation of the achievable precision of this method.

If Ω_{spec} determinations are made using a Cary 400 or comparable spectrophotometer, then the value of ${}_{235}\varepsilon_{NO3}$ reported in Table 1 can be used directly in Eq. (4) to provide accurate Ω_{spec} values without further calibration. However, if Ω_{spec} determinations are made using an Agilent 8453 or comparable spectrophotometer, then user-determined instrument-specific apparent molar absorptivity coefficients (${}_{235}\varepsilon^{*}_{NO3}$) must be used. Small deviations in wavelength calibrations between spectrophotometers (±0.1 nm) can create large deviations in measured absorbances and, thereby, large errors in Ω_{spec}. The use of instrument-specific ${}_{\lambda}\varepsilon^{*}_{NO3}$values eliminates the problems associated with these small wavelength discrepancies. Whenever an instrument's wavelength scale is recalibrated, a new ${}_{235}\varepsilon^{*}_{NO3}$ must be determined for that instrument (as illustrated in Table 2). It is important to emphasize that after a one-time, instrument-specific characterization of ${}_{235}\varepsilon^{*}_{NO3}$, the spectrophotometric method developed here to determine carbonate saturation state is calibration-free. In addition, it is important to note that subnanomolar differences in wavelength calibrations are insignificant for spectrophotometric pH determinations because those absorbance measurements are made at the broad absorbance maxima of sulfonephthalein indicators.

The choice of which sulfonephthalein indicator to use for the pH absorbance measurements (mCP or cresol red) is crucial for accurate Ω_{spec} determinations. When $pH_1 > 7.8$, mCP must be used; when $pH_1 < 7.8$, CR is recommended. The choice of an indicator therefore requires some upfront knowledge of the likely seawater pH. The pH of most coastal and open

ocean waters is >7.8, so most measurements will utilize mCP. Cases where CR would likely be used include coastal upwelling regions, deep-water samples, and areas where microbial respiration is high.

The efficacy (i.e., precision or resolution) of the spectrophotometric saturation state measurements described in this work depend in large part on achieving a substantial difference between pH_1 and pH_2. However, the extent to which large pH differences can be measured spectrophometrically is limited by the small suite of well-characterized purified indicators. Currently, only mCP (pK ~8.0; [26]) and CR (pK ~7.8; [27]) meet the requisite criteria. Using larger nitric acid additions or more concentrated nitric acid in order to achieve $pH_2 < 6$ would likely significantly improve the precision and accuracy of the Ω_{spec} measurements. Implementation of this advancement, though, will require (a) thorough characterization of a lower-pK indicator (e.g., bromocresol purple, pK ~5.8; [37]) and (b) determination of ${}_{\lambda}\varepsilon^{*}_{NO3}$ at longer wavelengths to compensate for the larger absorbance values that would result from higher concentrations of nitric acid.

The spectrophotometric procedure developed in this work is also amenable to flow through and in situ applications. Because the mixing ratio of seawater and nitric acid is determined spectrophotometrically, the need for accurate volumetric metering of acid delivery is eliminated. The achievable in situ precision is directly dependent on the accuracy of the spectrophotometric measurements. Notably, because a single spectrophotometric cell would be used for any in situ analyses, absorbance errors associated with the manual manipulation of spectrophotometric cells (i.e., moving cells into and out of the spectrophotometers) would be eliminated, thereby improving Ω_{spec} precision and accuracy relative to benchtop measurements.

The development of procedures for in situ analysis will, of course, require characterization of the temperature and pressure dependencies of nitrate molar absorptivities.

Seawater carbonate saturation state determinations that require only spectrophotometric instrumentation, which is widely available and relatively inexpensive, creates new opportunities for simple, fast, and cost-effective monitoring of ocean acidification. Spectrophotometric measurements of saturation state are especially suitable for applications where the highest achievable precision and accuracy are not required. Potential applications include observations in coastal areas (where spatial and temporal variability are high) as well as the routine monitoring of seawater at fish hatcheries and shellfish farms.

Next Generation Photometers

First Generation DIY Photometer

Seawater pH is an important CO_2 system variable that is measured frequently in coastal and open ocean areas. It controls the speciation of biologically important metals and has a strong influence on biogeochemical processes. Current instruments which measure pH with adequate accuracy are expensive and require frequent calibrations. The inexpensive portable pH probes that are available don't provide sufficient accuracy, are often unreliable and also require frequent calibrations. This gap between what's needed and what's available inspired the creation of an inexpensive DIY photometer which measures pH with an accuracy of ±0.01 [62].

The photometer employs spectrophotometric techniques [26] to measure pH using inexpensive LEDS as the light source and mCP indicator dye to generate pH-dependent absorbance ratios. Using this technique, the mCP absorbance ratios are combined with salinity and temperature to calculate pH. All the parts can be purchased for < $100 and assembled with modest technical skill. A major advantage of this novel instrument is that it only requires a one-time calibration and then no subsequent field calibrations are necessary. This is of particular importance as instrument calibrations can be time intensive and costly to users. This first-generation photometer is suitable for operation by scientists and required additional measurements of salinity and temperature to calculate the pH. The next generation photometer described in this work answers the need for a more user-friendly model that can be operated by the public (i.e., non-scientists).

Next Generation Photometer

The structure of the next generation photometer has been updated for easy portability and handling (Figure 4).

Figure 4: Next generation photometer

It has a sample tube separated from the electrical components that holds approximately 100 ml of seawater. The LEDS and detector are housed within the sample tube (pathlength = 5.0 cm) along with a salinity and temperature probe. The addition of the salinity and temperature probe allows measurements and calculation of pH to be instantaneously performed with one

instrument. The tube also contains an indicator port for easy mCP indicator additions. Finally, a mobile application was created which connects the photometer via Bluetooth to an iPhone or iPad. The app allows the user to control the pH measurement with their device and conveniently store the data.

Modifications to the Hardware

There were several modifications made to the next generation photometer to increase the accuracy and efficiency of pH measurements. The structure within the sample tube was amended to create a more open design that maximized sample flow and efficient mixing of indicator solution and seawater. The pathlength was shortened from 10 cm to 5 cm to decrease the seawater sample size. This doubled the concentration of the indicator required for each pH measurement.

Initially the LEDS and detector were mounted with a clear epoxy (hysol #ES1902, Henkel AG & Company) to hold them in place. However, after repeated testing, the epoxy underwent severe discoloration and degradation. After trying multiple types of epoxy, it was found that eliminating the epoxy altogether and using a convex glass lens to cover the optical components was a much better solution.

Using convex glass also eliminated another major problem, bubbles. When operating the epoxy-based design, bubbles would often form within the light path, scattering light and causing inaccurate pH measurements. Initially, we experimented with different methods of adding seawater into the sample tube to diminish the occurrence of bubbles. It was determined that the optimal procedure for adding seawater samples was to tilt the instrument and pour slowly as if beer were being poured from a tap. In the end, the addition of convex coverings over the photometer's optical components solved this problem.

A serious recurring problem was constant drift in the salinity probes within the photometers. After a salinity probe was accurately calibrated, over a matter of hours salinity measurements would drift until they were more than 5 salinity units different (positive or negative) from the known salinity of a sample. The source of the drift was found to be interference between electrical components within the sample tube (i.e., detector, LEDS). To prevent this interference, the software was adjusted to alternate measurements of pH and salinity so that during an optical measurement or a salinity measurement, the electrical components of the other device were inactivated. In addition, the salinity probe was recessed within the sample tube – decreasing its proximity to the optical components. After those two modifications, the salinity probe values remained consistent.

Calibration Procedure

A one-time calibration of the absorbance ratios of each broad band LED photometer must be performed against the absorbance ratios obtained with a high-quality narrowband spectrophotometer. For every seawater sample, an absorbance ratio measured on the photometer (R_B) was coordinated with an absorbance ratio obtained with the narrowband spectrophotometer (R_N). To increase pH accuracy, each R_B value obtained with the photometer is converted to an R_N value using a coordinating equation. The requisite equation is generated via the calibration process and then entered into a photometer's software for use in all future measurements.

The calibration procedure for the next generation photometers is similar to the calibration procedure for the original instruments [62], but modified to allow mass calibration of many instruments at one time. Six calibration solutions of surface seawater were adjusted so that their pHs spanned the range $7.2 < pH < 8.2$ at approximately equal intervals. Adjustments were made with additions of 1.0 N HCl or 1.0 N NaOH and mCP indicator was then added to the solution

samples (~3.3 µM). The absorbance ratios of each calibration solution were measured on the photometer and spectrophotometer (Agilent 8453). These measurements were made simultaneously so the temperature was constant. The R_B and R_N values were then plotted against each other to generate a linear or polynomial equation.

Figure 5 shows the calibration plot and equation for a photometer designated as unit 115. The R^2 value was 0.9971, showing that the equation provided a good description of the data. The regression equation was input into the unit's software for facile pH calibrations.

$$R_N = 0.0679(R_B)^2 + 0.8783R_B + 0.0021 \quad (16)$$

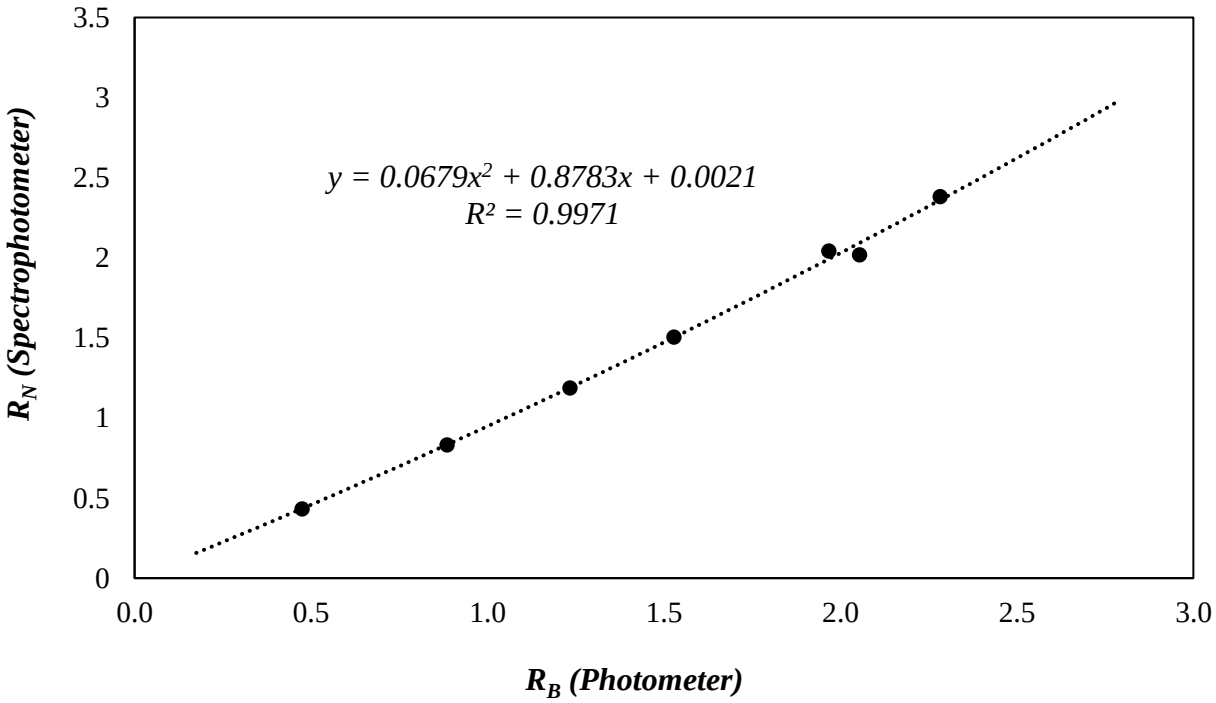

Figure 5: Absorbance ratios of unit 115 (R_B) plotted against absorbance ratios obtained with an Agilent 8453 spectrophotometer (R_N). The absorbance ratios of calibration solutions ranged $0.4 < R_B < 2.4$.

Testing the Calibration

After a unit is successfully calibrated, the calibration is evaluated by direct comparisons of photometer pH and spectrophotometer pH using identical seawater samples. The accuracy goal for each photometer is pH measurements with an accuracy of ±0.01. Up to now, three units with the most up to date modifications have been calibrated and tested. The best of the units, unit 115, measured pH within ± 0.01 for 12 of 15 measurements, and all 15 measurements were within ±0.02.

Future steps for the Next Generation Photometers

The pH measurements made with unit 115 suggest that these photometers can attain the accuracy goal of ± 0.01. Construction of 10–20 fully functional additional units is required to provide a robust assessment of the current photometer design.

The final stage of the pH photometer project will be to put these units in the hands of middle and high school students, citizen scientists, and other interested groups (e.g., resource managers) so that a substantial spatial density of pH measurements is created each day in and around Tampa Bay. Measurements in the field will be preceded by a thorough period of classroom teaching to ensure that users know how to operate the photometers properly and understand the implications of their measurements. All photometer apps will eventually be connected to a central database so that anyone can log onto the website and view the hundreds and potentially thousands of pH measurements made in the coastal environment each week. This project not only increases accurate monitoring of ocean acidification but also provides an avenue for students and citizens to get hands-on familiarity with quantitative ocean science. As such, these pH photometers can be used as teaching tools to increase awareness of the issues that face our ocean and get people excited about conservation.

Lessons Learned

Spectrophotometric Saturation State Measurements

While refining the carbonate measurement protocol we developed additional guidelines to help ensure optimal precision and accuracy in measured saturation states.

First, to obtain accurate pH and nitrate absorbance measurements, the baseline shifts (absorbance measured at 730 and 385 nm) should not be larger than ±0.004.

Second, for measurments performed using mCP, cell 2 should be acidified so that pH_2 is within the range 7.15–7.30. For pH_2 >7.30, the difference between the initial and final pH may be too small to provide accurate measurements, and for pH_2 <7.15, the pH may be too far outside the ideal indicating range of mCP (approximately 7.2 < pH < 8.2) to provide accurate measurements. In order to assess the magnitude of HNO_3 additions required to achieve optimum values of pH_2, it is useful to calculate pH_1 prior to the acid addition. This can be easily done using an excel sheet that contains the appropriate equations for calculating pH from absorbance measurements.

Finally, solution temperatures during all measurements should be maintained within 25°C ±0.5°C. Nitrate molar absorptivity coefficients are temperature sensitive, so large temperature deviations will cause calculated ΔNO_3^-, and consequently Ω_{spec}, to be overestimated or underestimated. To prevent offsets due to temperature deviations, test cells containing seawater should be equilibrated within thermostatted compartments prior to measurements.

Photometers

Next generation photometers are intended for use in the field, so care must be taken to ensure that field conditions do not affect measurement accuracy. For example, if the temperature of the photometer itself (i.e., the plastic sample compartment, detector, and LEDs) is substantially different from the in situ seawater temperature, it can perturb the temperature of added seawater. This can occur if the photometer heats up in the sun and then is immediately used to measure pH. To address this effect, we recommend cooling the photometer with seawater prior to the final pH measurement of a sample so the cell-compartment temperature is close to the temperature of the in situ seawater. Variations in the temperature of the photometer's LEDS and detector can also affect absorbance measurements. We recommend that photometers are not left in direct sunlight or set on hot surfaces for prolonged periods of time.

Future Research Needs

Spectrophotometric Saturation State Measurements

The salinity range of the seawater used in this work ($34.2 < S < 36.4$) was typical of open ocean seawater. Measurements over a wider salinity range, especially including coastal waters ($20 \leq S \leq 30$), should be made to further demonstrate the efficacy of the measurement protocol.`

Measurements in the presence of high suspended particle loading can potentially have an adverse impact on precision and accuracy. Although baseline measurements should substantially diminish (correct for) potential interferences from suspended matter and colored tannins, experiments should be performed to assess the influence of both light scattering and colored dissolved organic matter on measurement precision and accuracy

In the absence of direct measurements of calcium concentrations, the accuracy of calculated carbonate saturation states is dependent on the proportionality between $[Ca^{2+}]_T$ and salinitiy. In coastal environments along the west coast of Florida, for example, substantial $[Ca^{2+}]_T/S$ variations can be observed due to high calcium concentrations within karstic springwaters that flow out and mix with neighboring coastal waters. This effect generally leads to underestimates of carbonate saturation states unless calcium concentrations are directly measured. Calcium concentration enhancements are especially important at low salinities, and may necessitate regional evaluations of $[Ca^{2+}]_T/S$ variations in some coastal environments. Another potentially significant effect on calculated carbonate saturation states in coastal waters is high levels of organic contributions to total alkalinity. This effect is not currently accounted for in calculations of CO_2 system parameters (including saturation states) that are derived from

measurements of A_T and C_T. It would be valuable to assess the magnitude of this effect by comparing saturation states derived from A_T and C_T to saturation states calculated from measurements of C_T and in situ pH.

Photometers

Evaluations to date have confirmed that calibrated photometers can attain a pH accuracy of 0.01 compared to measurements obtained using high quality spectrophotometers. However, further testing is required to determine the stability of calibrations over months and even years. In addition, as previously noted, in conjunction with increased use of pH photometers in coastal environments, further assessment of the effects of suspended matter and dissolved colored organic matter on pH measurements is advisable. Finally, implementation of an easy and accurate mass-calibration procedure will become increasingly important as numerous instruments are constructed and utilized in the field.

References

[1] P. Tans, R. Keeling, Trends in atmospheric carbon dioxide, (2014). Available from: http://www.esrl.noaa.gov/gmd/ccgg/trends/

[2] C. Le Quéré, R. Moriarty, R.M. Andrew, J.G. Canadell, S. Sitch, J.I. Korsbakken, P. Friedlingstein, G.P. Peters, R.J. Andres et al., Global Carbon Budget 2015, Earth System Science Data. 7 (2015) 349–396.

[3] C.L. Sabine, R.A. Feely, N. Gruber, R.M. Key, K. Lee, J.L. Bullister, R. Wanninkhof, C.S. Wong, D.W.R. Wallace, B. Tilbrook, F.J. Millero, T.-H. Peng, A. Kozyr, T. Ono, A.F. Rios, The oceanic sink for anthropogenic CO_2., Science. 305 (2004) 367–71.

[4] K. Caldeira, M.E. Wickett, Oceanography: Anthropogenic carbon and ocean pH, Nature. 425 (2003) 365–365.

[5] K. Caldeira, M.E. Wickett, Ocean model predictions of chemistry changes from carbon dioxide emissions to the atmosphere and ocean, J. Geophys. Res. 110 (2005) C09S04.

[6] J.C. Orr, V.J. Fabry, O. Aumont, L. Bopp, S.C. Doney, R.A. Feely, A. Gnanadesikan, N. Gruber, A. Ishida, F. Joos, R.M. Key, K. Lindsay, E. Maier-Reimer, R. Matear, P. Monfray, A. Mouchet, R.G. Najjar, G.-K. Plattner, K.B. Rodgers, C.L. Sabine, J.L. Sarmiento, R. Schlitzer, R.D. Slater, I.J. Totterdell, M.-F. Weirig, Y. Yamanaka, A. Yool, Anthropogenic ocean acidification over the twenty-first century and its impact on calcifying organisms, Nature. 437 (2005) 681–686.

[7] M.D. Iglesias-Rodriguez, P.R. Halloran, R.E.M. Rickaby, I.R. Hall, E. Colmenero-Hidalgo, J.R. Gittins, D.R.H. Green, T. Tyrrell, S.J. Gibbs, P. von Dassow, E. Rehm, E. V.

Armbrust, K.P. Boessenkool, Phytoplankton Calcification in a High-CO_2 World, Science (80). 320 (2008) 336–340.

[8] A.D. Moy, W.R. Howard, S.G. Bray, T.W. Trull, Reduced calcification in modern Southern Ocean planktonic foraminifera, Nature Geoscience 2 (2009) 276–280.

[9] J.P. Gattuso, M. Frankignoulle, I. Bourge, S. Romaine, R.W. Buddemeier, Effect of calcium carbonate saturation of seawater on coral calcification, Global and Planetary Change. 18 (1998) 37–46.

[10] C. Langdon, T. Takahashi, C. Sweeney, D. Chipman, J. Goddard, F. Marubini, H. Aceves, H. Barnett, M.J. Atkinson, Effect of calcium carbonate saturation state on the calcification rate of an experimental coral reef, Global Biogeochem. Cycles. 14 (2000) 639–654.

[11] G.G. Waldbusser, B. Hales, C.J. Langdon, B.A. Haley, P. Schrader, E.L. Brunner, M.W. Gray, C.A. Miller, I. Gimenez, Saturation-state sensitivity of marine bivalve larvae to ocean acidification, Nat. Clim. Chang. 5 (2014) 273–280.

[12] B. Gaylord, T.M. Hill, E. Sanford, E.A. Lenz, L.A. Jacobs, K.N. Sato, A.D. Russell, A. Hettinger, Functional impacts of ocean acidification in an ecologically critical foundation species, J. Exp. Biol. 214 (2011) 2586–2594.

[13] N. Bednaršek, G.A. Tarling, D.C.E. Bakker, S. Fielding, E.M. Jones, H.J. Venables, P. Ward, A. Kuzirian, B. Lézé, R.A. Feely, E.J. Murphy, Extensive dissolution of live pteropods in the Southern Ocean, Nat. Geosci. 5 (2012) 881–885.

[14] N. Bednaršek, G.A. Tarling, D.C.E. Bakker, S. Fielding, R.A. Feely, Dissolution Dominating Calcification Process in Polar Pteropods Close to the Point of Aragonite Undersaturation, PLoS One. 9 (2014) e109183.

[15] V. Fabry, J. McClintock, J. Mathis, J. Grebmeier, Ocean Acidification at High Latitudes:

The Bellwether, Oceanography. 22 (2009) 160–171.

[16] R.A. Feely, S.C. Donet, S.R. Cooley, Ocean Acidification: Present Conditions and Future Changes in a High-CO_2 World, Oceanography. 22 (2009) 36–47.

[17] C.M. Duarte, I.E. Hendriks, T.S. Moore, Y.S. Olsen, A. Steckbauer, L. Ramajo, J. Carstensen, J.A. Trotter, M. Mcculloch, C.M. Duarte, I.E. Hendriks:, T.S. Moore, Y.S. Olsen, A. Steckbauer, : L Ramajo, L. Ramajo, J. Carstensen, J.A. Trotter, M. Mcculloch, Is Ocean Acidification an Open-Ocean Syndrome? Understanding Anthropogenic Impacts on Seawater pH, Estuaries and Coasts. 36 (2013) 221–236.

[18] R.A. Feely, S.R. Alin, J. Newton, C.L. Sabine, M. Warner, A. Devol, C. Krembs, C. Maloy, The combined effects of ocean acidification, mixing, and respiration on pH and carbonate saturation in an urbanized estuary, Estuar. Coast. Shelf Sci. 88 (2010) 442–449.

[19] S.L. Garrard, M.C. Gambi, M.B. Scipione, F.P. Patti, M. Lorenti, V. Zupo, D.M. Paterson, M.C. Buia, Indirect effects may buffer negative responses of seagrass invertebrate communities to ocean acidification, J. Exp. Mar. Bio. Ecol. 461 (2014) 31–38.

[20] V. Fabry, B. Seibel, R. Feely, J. Orr, Impacts of ocean acidification on marine fauna and ecosystem processes, ICES J. Mar. Sci. 65 (2008) 414–432.

[21] A. Dickson, C. Sabine, J. Christian, Guide to best practices for ocean CO_2 measurements, PICES Special Publication: Sidney, BC, Canada. 3 (2007).

[22] A.G. Dickson, The measurement of sea water pH, Marine Chemistry. 44 (1993) 131–142.

[23] G.L. Robert-Baldo, M.J. Morris, R.H. Byrne, Spectrophotometric determination of seawater pH using phenol red, Anal. Chem. 57 (1985) 2564–2567.

[24] R.H. Byrne, G.L. Robert-Baldo, S.W. Thompson, C.T.. Chen, Seawater pH measurements: an at-sea comparison of spectrophotometric and potentiometric methods,

Deep Sea Res. Part A. Oceanogr. Res. Pap. 35 (1988) 1405–1410.

[25] R.H. Byrne, J.A. Breland, High precision multiwavelength pH determinations in seawater using cresol red, Deep Sea Res. Part A, Oceanogr. Res. Pap. 36 (1989) 803–810.

[26] T.D. Clayton, R.H. Byrne, Spectrophotometric seawater pH measurements : total hydrogen results, Deep. Res. 40 (1993) 2115–2129.

[27] M.C. Patsavas, R.H. Byrne, X. Liu, Physical-chemical characterization of purified cresol red for spectrophotometric pH measurements in seawater, Mar. Chem. 155 (2013) 158–164.

[28] H. Zhang, R.H. Byrne, Spectrophotometric pH measurements of surface seawater at in-situ conditions: absorbance and protonation behavior of thymol blue, Mar. Chem. 52 (1996) 17–25.

[29] K. Shitashima, M. Kyo, Y. Koike, H. Henmi, Development of in situ pH sensor using ISFET, in: Proc. (2002) Interntional Symp. Underw. Technol. (Cat. No.02EX556), IEEE, n.d.: pp. 106–108.

[30] K. Shitashima, Evolution of compact electrochemical in-situ pH-pCO_2 sensor using ISFET-pH electrode, MTS/IEEE Seattle, Ocean. 2010. (2010) 2–6.

[31] T.R. Martz, J.G. Connery, K.S. Johnson, Testing the Honeywell Durafet® for seawater pH applications, Limnol. Oceanogr. Methods. 8 (2010) 172–184.

[32] R.H. Byrne, X. Liu, E.A. Kaltenbacher, K. Sell, Spectrophotometric measurement of total inorganic carbon in aqueous solutions using a liquid core waveguide, Anal. Chim. Acta. 451 (2002) 221–229.

[33] C. Culberson, Seawater alkalinity determination by the pH method., J. Mar. Res. 28 (1970) 15–21.

[34] A.L. Bradshaw, P.G. Brewer, D.K. Shafer, R.T. Williams, Measurements of total carbon dioxide and alkalinity by potentiometric titration in the GEOSECS program, Earth Planet. Sci. Lett. 55 (1981) 99–115.

[35] A.L. Bradshaw, P.G. Brewer, High precision measurements of alkalinity and total carbon dioxide in seawater by potentiometric titration. 2. Measurements on standard solutions, Mar. Chem. 24 (1988) 155–162.

[36] F.J. Millero, J.Z. Zhang, K. Lee, D.M. Campbell, Titration alkalinity of seawater, Mar. Chem. 44 (1993) 153–165.

[37] W. Yao, R.H. Byrne, Simplified seawater alkalinity analysis: Use of linear array spectrometers, Deep. Res. Part I Oceanogr. Res. Pap. 45 (1998) 1383–1392.

[38] R.H. Byrne, W. Yao, Procedures for measurement of carbonate ion concentrations in seawater by direct spectrophotometric observations of Pb(II) complexation, Mar. Chem. 112 (2008) 128–135.

[39] J. Canadell, C. Le Quéré, Contributions to accelerating atmospheric CO_2 growth from economic activity, carbon intensity, and efficiency of natural sinks, Proc. Natl. Acad. Sci. 104 (2007) 18866–18879.

[40] R.A. Feely, C.L. Sabine, K. Lee, W. Berelson, J. Kleypas, V.J. Fabry, F.J. Millero, Impact of anthropogenic CO_2 on the $CaCO_3$ system in the oceans, Science (80-.). 305 (2004) 362–366.

[41] R.A. Feely, C.L. Sabine, R.H. Byrne, F.J. Millero, A.G. Dickson, R. Wanninkhof, A. Murata, L.A. Miller, D. Greeley, Decadal changes in the aragonite and calcite saturation state of the Pacific Ocean, Global Biogeochem. Cycles. 26 (2012) 1–15.

[42] S.C. Doney, V.J. Fabry, R.A. Feely, J.A. Kleypas, Ocean Acidification: The Other CO_2

Problem, Ann. Rev. Mar. Sci. 1 (2009) 169–192.

[43] M.D. DeGrandpre, T.R. Martz, R.D. Hart, D.M. Elison, A. Zhang, A.G. Bahnson, Universal Tracer Monitored Titrations, Anal. Chem. 83 (2011) 9217–9220.

[44] R.S. Spaulding, M.D. DeGrandpre, J.C. Beck, R.D. Hart, B. Peterson, E.H. De Carlo, P.S. Drupp, T.R. Hammar, Autonomous in Situ Measurements of Seawater Alkalinity, Environ. Sci. Technol. 48 (2014) 9573–9581.

[45] A.G. Dickson, C. Goyet, Handbook of methods for the analysis of the various parameters of the carbon dioxide system in sea water, ORNL/CDIAC-74. (1994).

[46] F.J. Millero, A. Poisson, International one-atmosphere equation of state of seawater, Deep Sea Res. Part A. Oceanogr. Res. Pap. 28 (1981) 625–629.

[47] F.J. Millero, R. Feistel, D. Wright, The composition of Standard Seawater and the definition of the Reference-Composition Salinity Scale, Deep Sea Res. Part I Oceanogr. Res. Pap. 55 (2008) 50–72.

[48] Agilent Technologies, Agilent Cary 4000/5000/6000i Series UV-Vis-NIR Guaranteed Specifications, 2011. http://hpst.cz/sites/default/files/uploaded_files/cary_4000_5000_6000i_specifikace.pdf (accessed September 21, 2017).

[49] Agilent Technologies, Agilent 8453 UV-visible spectrophotometer – UV-visible spectroscopy solutions for pharmaceutical analysis, 2008. http://cn.agilent.com/cs/library/brochures/5989-8681EN.pdf (accessed September 21, 2017).

[50] M.C. Patsavas, R.H. Byrne, X. Liu, Purification of meta-cresol purple and cresol red by flash chromatography: Procedures for ensuring accurate spectrophotometric seawater pH

measurements, Mar. Chem. 150 (2013) 19–24.

[51] D.C. Harris, Quantitative chemical analysis, W.H. Freeman and Co, 2007.

[52] D. Pierrot, E. Lewis, D. Wallace, CO2SYS DOS Program developed for CO_2 system calculations, Carbon Dioxide Information Analysis Center, Oak Ridge National Laboratory, US, Department of Energy: Oak Ridge, TN. (2006).

[53] T. Lueker, A. Dickson, C. Keeling, Ocean pCO_2 calculated from dissolved inorganic carbon, alkalinity, and equations for K_1 and K_2: validation based on laboratory measurements of CO_2 in gas and, Mar. Chem. 70 (2000) 105–119.

[54] A. Dickson, Thermodynamics of the dissociation of boric acid in synthetic seawater from 273.15 to 318.15 K, Deep Sea Res. Part A. Oceanogr. Res. 37 (1990) 755–766.

[55] F.J. Millero, Thermodynamics of the carbon dioxide system in the oceans, Geochim. Cosmochim. Acta. 59 (1995) 661–677.

[56] M. Alfonso, The solubility of calcite and aragonite in seawater at various salinities, temperatures, and one atmosphere total pressure, Am. J. Sci. 283 (1983) 780–799.

[57] A.G. Dickson, Standard potential of the reaction: AgCl(s) + 1 2H2(g) = Ag(s) + HCl(aq), and and the standard acidity constant of the ion HSO_4^- in synthetic sea water fromj 273.15 to 318.15 K, J. Chem. Thermodyn. 22 (1990) 113–127.

[58] L.R. Uppström, The boron/chlorinity ratio of deep-sea water from the Pacific Ocean, Deep Sea Res. Oceanogr. 21 (1974) 161–162.

[59] X. Liu, M.C. Patsavas, R.H. Byrne, Purification and Characterization of meta Cresol Purple for Spectrophotometric Seawater pH Measurements, Environ. Sci. Technol. 45 (2011) 4862–4868.

[60] I. Kolthoff, E. Sandell, E. Meehan, S. Bruckenstein, Quantitative chemical analysis, 4th ed.

The Macmillan Co., London, 1969, p. 1157.

[61] J. Newton, R. Feely, E. Jewett, P. Williamson, Global ocean acidification observing network: requirements and governance plan. GOA-ON, (2014). http://www.goa-on.org/GOA-ON.php

[62] B. Yang, M.C. Patsavas, R.H. Byrne, J. Ma, Seawater pH measurements in the field: A DIY photometer with 0.01 unit pH accuracy, Mar. Chem. 160 (2014) 75–81.

Appendix A: Metadata for Carbonate Saturation State Measurements

Table A5: Sample information for spectrophotometric saturation state measurements on all instruments

Salinity	TA	pH_1	ΔNO_3^- (µmol/Kg)	pH_2	θ	C_T (µmol/Kg)	A_{T1} (µmol/Kg)	Ω_{spec}	Ω_{calc}
Spectrophotometer 1									
36.043	2382.9	7.940	283.6	7.236	0.99938	2187.6	2446.1	3.01	2.93
36.043	2382.9	7.945	283.0	7.220	0.99938	2104.4	2359.1	2.92	2.96
36.043	2382.9	7.943	330.4	7.080	0.99927	2125.2	2380.6	2.94	2.95
36.043	2382.9	7.941	288.4	7.196	0.99937	2102.4	2354.9	2.90	2.94
36.043	2382.9	7.941	253.2	7.324	0.99944	2160.3	2417.1	2.98	2.93
36.043	2382.9	7.941	303.3	7.158	0.99933	2125.2	2379.6	2.93	2.94
36.043	2382.9	7.945	301.4	7.172	0.99934	2133.8	2390.8	2.96	2.95
36.043	2382.9	7.948	315.0	7.125	0.99931	2099.5	2355.8	2.94	2.97
36.043	2382.9	7.941	321.4	7.091	0.99929	2091.0	2342.4	2.88	2.93
36.043	2382.9	7.937	298.7	7.158	0.99934	2107.0	2357.5	2.88	2.91
36.043	2382.9	7.937	305.2	7.142	0.99933	2120.1	2371.3	2.90	2.91
36.043	2382.9	7.942	310.6	7.120	0.99932	2078.6	2329.4	2.87	2.94
36.043	2382.9	7.934	314.3	7.115	0.99931	2135.3	2386.0	2.90	2.90
36.043	2382.9	7.943	310.1	7.135	0.99932	2113.0	2367.1	2.92	2.94
36.043	2382.9	7.943	319.3	7.119	0.99930	2144.5	2401.5	2.97	2.95
36.043	2382.9	7.943	305.1	7.147	0.99933	2102.4	2355.8	2.91	2.94
36.043	2382.9	7.942	320.9	7.094	0.99929	2092.3	2344.1	2.89	2.94
36.043	2382.9	7.939	297.2	7.167	0.99935	2112.5	2364.4	2.90	2.92
36.043	2382.9	7.948	311.5	7.122	0.99932	2061.8	2315.0	2.89	2.97
36.043	2382.9	7.942	296.5	7.177	0.99935	2119.7	2373.7	2.93	2.94
36.093	2382.9	7.888	266.3	7.203	0.99941	2205.6	2435.9	2.72	2.66
36.093	2382.9	7.886	265.6	7.185	0.99942	2148.5	2373.5	2.64	2.65
36.093	2382.9	7.894	266.5	7.192	0.99941	2135.9	2364.3	2.67	2.69
36.093	2382.9	7.889	279.7	7.166	0.99939	2214.8	2445.8	2.73	2.66
36.093	2382.9	7.890	254.5	7.236	0.99944	2185.8	2415.4	2.70	2.67
36.093	2382.9	7.886	271.0	7.178	0.99940	2179.5	2406.7	2.68	2.65
36.093	2382.9	7.882	253.4	7.228	0.99944	2191.2	2417.1	2.67	2.63
36.093	2382.9	7.883	269.1	7.195	0.99941	2239.5	2468.9	2.73	2.63
36.093	2382.9	7.881	282.3	7.150	0.99938	2228.9	2456.4	2.70	2.62

Salinity	TA	pH_1	ΔNO_3^- (µmol/Kg)	pH_2	θ	C_T (µmol/Kg)	A_{T1} (µmol/Kg)	Ω_{spec}	Ω_{calc}
36.093	2382.9	7.881	267.1	7.191	0.99941	2218.2	2445.0	2.69	2.62
36.093	2382.9	7.887	262.6	7.191	0.99942	2132.7	2357.1	2.62	2.65
36.093	2382.9	7.888	245.4	7.255	0.99946	2164.6	2391.7	2.67	2.66
36.093	2382.9	7.887	268.2	7.191	0.99941	2193.3	2421.9	2.70	2.65
36.093	2382.9	7.887	274.7	7.153	0.99940	2133.0	2357.3	2.62	2.65
36.093	2382.9	7.888	261.4	7.210	0.99943	2180.8	2408.9	2.69	2.66
36.093	2382.9	7.896	259.1	7.221	0.99943	2143.8	2374.1	2.69	2.70
36.093	2382.9	7.894	272.7	7.156	0.99940	2083.0	2307.5	2.60	2.69
36.093	2382.9	7.889	262.0	7.190	0.99942	2112.9	2337.0	2.61	2.66
36.093	2382.9	7.890	258.9	7.229	0.99943	2205.5	2436.7	2.73	2.67
36.093	2382.9	7.863	254.8	7.168	0.99944	2108.6	2318.6	2.46	2.53
36.093	2382.9	7.860	250.1	7.197	0.99945	2179.8	2392.6	2.53	2.52
36.093	2382.9	7.857	267.2	7.148	0.99941	2202.1	2415.1	2.54	2.51
36.093	2382.9	7.856	259.2	7.151	0.99943	2138.0	2345.9	2.46	2.50
36.093	2382.9	7.857	258.8	7.176	0.99943	2217.3	2430.8	2.55	2.50
36.093	2382.9	7.865	249.1	7.200	0.99945	2146.7	2360.2	2.52	2.54
36.387	2403.1	8.061	270.1	7.487	0.99941	2046.5	2372.8	3.64	3.69
36.387	2403.1	8.058	390.7	7.120	0.99914	2104.4	2435.3	3.72	3.67
36.387	2403.1	8.068	411.4	7.063	0.99910	2068.0	2401.6	3.73	3.73
36.387	2403.1	8.060	335.3	7.271	0.99926	2035.9	2360.7	3.61	3.68
36.387	2403.1	8.055	358.2	7.226	0.99921	2134.9	2466.6	3.75	3.65
36.387	2403.1	8.061	391.6	7.111	0.99914	2076.5	2406.2	3.69	3.69
36.387	2403.1	8.068	389.3	7.138	0.99914	2089.5	2425.4	3.77	3.73
36.387	2403.1	8.064	365.4	7.169	0.99920	2009.2	2333.6	3.59	3.71
36.387	2403.1	8.059	396.4	7.113	0.99913	2127.3	2460.9	3.77	3.67
36.378	2403.1	8.037	380.2	7.091	0.99916	2069.0	2381.0	3.50	3.53
36.378	2403.1	8.036	378.0	7.089	0.99917	2050.1	2359.9	3.46	3.53
36.378	2403.1	8.036	337.1	7.229	0.99926	2077.3	2390.1	3.51	3.53
36.378	2403.1	8.036	368.4	7.120	0.99919	2055.4	2365.5	3.47	3.53
36.378	2403.1	8.039	345.9	7.185	0.99924	2024.2	2333.6	3.44	3.55
36.378	2403.1	8.037	351.0	7.172	0.99923	2044.8	2354.6	3.46	3.53
36.378	2403.1	8.038	384.9	7.084	0.99915	2077.6	2391.7	3.53	3.54
36.378	2403.1	8.039	308.5	7.330	0.99932	2082.0	2397.3	3.54	3.55
36.378	2403.1	8.044	365.5	7.138	0.99920	2039.4	2353.1	3.50	3.58
36.378	2403.1	8.036	311.6	7.319	0.99931	2100.0	2414.7	3.55	3.53
36.378	2403.1	8.039	336.1	7.236	0.99926	2074.1	2388.4	3.53	3.55
36.378	2403.1	8.039	346.4	7.238	0.99924	2163.2	2486.5	3.68	3.55
36.378	2403.1	8.036	339.3	7.237	0.99925	2122.5	2439.3	3.58	3.53
36.378	2403.1	8.028	329.9	7.254	0.99927	2129.3	2441.8	3.54	3.48
36.378	2403.1	8.036	338.3	7.253	0.99926	2155.5	2475.7	3.64	3.53
36.378	2403.1	8.045	328.3	7.282	0.99928	2091.4	2411.6	3.60	3.59

Salinity	TA	pH_1	ΔNO_3^- (µmol/Kg)	pH_2	θ	C_T (µmol/Kg)	A_{T1} (µmol/Kg)	Ω_{spec}	Ω_{calc}
36.378	2403.1	8.049	295.5	7.370	0.99935	2015.5	2330.4	3.50	3.61
36.378	2403.1	8.039	330.0	7.257	0.99927	2074.3	2388.8	3.53	3.55
36.378	2403.1	8.033	316.5	7.304	0.99930	2123.8	2438.9	3.56	3.51
36.378	2403.1	8.033	327.8	7.254	0.99928	2082.9	2394.3	3.50	3.51
36.378	2403.1	8.033	317.7	7.307	0.99930	2142.4	2459.3	3.59	3.51
36.378	2403.1	8.033	318.9	7.297	0.99930	2123.2	2438.2	3.56	3.51
36.378	2403.1	8.037	337.6	7.234	0.99926	2089.4	2404.1	3.54	3.54
36.378	2403.1	8.033	302.1	7.344	0.99934	2106.9	2420.1	3.53	3.51
36.378	2403.1	8.038	303.5	7.345	0.99933	2087.8	2402.6	3.54	3.54
36.378	2403.1	8.036	301.7	7.345	0.99934	2081.0	2394.1	3.52	3.53
36.378	2403.1	8.045	312.2	7.316	0.99931	2046.4	2361.6	3.52	3.58
36.378	2403.1	8.036	321.6	7.276	0.99929	2073.3	2385.4	3.50	3.53
36.378	2403.1	8.033	309.3	7.320	0.99932	2100.6	2413.5	3.53	3.51
36.378	2403.1	8.036	316.3	7.289	0.99930	2058.3	2369.2	3.48	3.53
36.378	2403.1	8.034	310.4	7.330	0.99932	2131.2	2448.0	3.59	3.52
36.378	2403.1	8.035	314.4	7.322	0.99931	2138.2	2456.5	3.61	3.53
36.378	2403.1	8.035	312.4	7.314	0.99931	2101.3	2415.6	3.54	3.52
Spectrophotometer 2									
34.230	2260.1	7.998	309.2	7.169	0.99932	1995.6	2259.6	3.03	3.03
34.230	2260.1	8.003	267.7	7.322	0.99941	2003.5	2271.1	3.07	3.05
34.230	2260.1	8.003	337.0	7.086	0.99926	1985.2	2251.4	3.04	3.05
34.230	2260.1	8.003	318.8	7.145	0.99930	1992.0	2258.4	3.05	3.05
34.230	2260.1	8.001	314.8	7.150	0.99931	1981.1	2245.4	3.02	3.04
34.230	2260.1	7.997	317.4	7.142	0.99930	2000.3	2264.1	3.03	3.02
34.230	2260.1	8.000	320.9	7.133	0.99929	1995.6	2260.4	3.03	3.03
34.230	2260.1	7.998	313.7	7.153	0.99931	1992.1	2255.8	3.02	3.03
34.230	2260.1	8.001	317.9	7.148	0.99930	2001.3	2267.4	3.05	3.04
34.230	2260.1	8.020	318.7	7.176	0.99930	1983.0	2259.2	3.15	3.15
34.230	2260.1	8.022	328.5	7.156	0.99928	2004.4	2283.7	3.20	3.16
34.230	2260.1	8.023	313.0	7.210	0.99931	2008.6	2288.4	3.20	3.16
34.230	2260.1	8.022	305.4	7.215	0.99933	1960.4	2235.3	3.12	3.16
34.230	2260.1	8.020	331.3	7.127	0.99927	1968.0	2242.2	3.12	3.15
34.230	2260.1	8.019	319.1	7.167	0.99930	1970.8	2245.1	3.12	3.14
34.230	2260.1	8.016	316.2	7.182	0.99930	1999.4	2274.2	3.14	3.12
34.230	2260.1	8.024	317.0	7.189	0.99930	1982.5	2260.8	3.17	3.17
34.230	2260.1	8.023	305.0	7.226	0.99933	1978.8	2256.1	3.16	3.16
34.230	2260.1	8.022	323.5	7.165	0.99929	1985.7	2263.2	3.16	3.16
34.230	2260.1	8.015	324.0	7.147	0.99929	1981.6	2254.4	3.11	3.12
34.230	2260.1	8.017	313.6	7.191	0.99931	1997.4	2272.7	3.15	3.13
34.230	2260.1	8.012	305.8	7.211	0.99933	2006.6	2279.6	3.13	3.10
34.230	2260.1	8.015	310.8	7.190	0.99932	1977.3	2249.9	3.11	3.12

Salinity	TA	pH_1	ΔNO_3^- (µmol/Kg)	pH_2	θ	C_T (µmol/Kg)	A_{T1} (µmol/Kg)	Ω_{spec}	Ω_{calc}
34.230	2260.1	8.012	319.0	7.167	0.99930	2004.6	2277.7	3.13	3.10
36.378	2406.4	7.427	209.4	7.242	0.99954	2389.6	2427.5	1.06	1.05
36.378	2406.4	7.430	244.4	7.174	0.99946	2386.9	2425.8	1.07	1.06
36.378	2406.4	7.438	234.7	7.194	0.99948	2360.6	2402.4	1.07	1.08
36.378	2406.4	7.429	245.7	7.172	0.99946	2394.6	2433.4	1.07	1.06
36.378	2406.4	7.430	268.5	7.123	0.99941	2355.6	2394.4	1.05	1.06
36.378	2406.4	7.432	265.7	7.131	0.99941	2359.5	2399.2	1.06	1.06
36.378	2406.4	7.432	242.2	7.174	0.99947	2354.1	2393.9	1.06	1.06
36.378	2406.4	7.442	255.4	7.161	0.99944	2385.5	2428.8	1.10	1.09
36.378	2406.4	7.463	241.9	7.190	0.99947	2321.5	2371.9	1.12	1.14
36.378	2406.4	7.452	250.5	7.175	0.99945	2376.3	2423.0	1.12	1.11
36.378	2406.4	7.451	249.0	7.177	0.99945	2373.1	2419.7	1.11	1.11
36.378	2406.4	7.456	232.0	7.213	0.99949	2366.5	2414.8	1.12	1.12
36.378	2406.4	7.463	242.7	7.195	0.99946	2358.6	2409.2	1.14	1.14
36.378	2406.4	7.464	246.2	7.190	0.99946	2364.9	2415.9	1.14	1.14
36.378	2406.4	7.471	254.2	7.176	0.99944	2348.6	2402.0	1.15	1.16
36.378	2406.4	7.476	249.7	7.190	0.99945	2356.1	2411.4	1.17	1.17
36.378	2406.4	7.483	241.4	7.214	0.99947	2369.7	2427.6	1.20	1.18
34.830	2300.4	7.426	244.6	7.157	0.99944	2322.8	2355.7	1.00	0.98
34.830	2300.4	7.423	229.0	7.178	0.99948	2285.9	2317.5	0.98	0.97
34.830	2300.4	7.423	225.1	7.188	0.99949	2295.7	2327.5	0.99	0.98
34.830	2300.4	7.422	224.5	7.189	0.99949	2300.5	2331.8	0.98	0.97
34.830	2300.4	7.425	235.6	7.166	0.99946	2283.7	2316.1	0.99	0.98
34.830	2300.4	7.425	236.4	7.176	0.99946	2345.9	2378.2	1.01	0.98
34.830	2300.4	7.426	238.2	7.162	0.99946	2285.4	2318.2	0.99	0.98
34.830	2300.4	7.429	248.0	7.142	0.99943	2268.3	2301.8	0.99	0.99
34.830	2300.4	7.427	242.6	7.155	0.99945	2287.3	2320.3	0.99	0.98
34.775	2296.7	7.948	268.2	7.235	0.99939	2047.9	2290.9	2.81	2.82
34.775	2296.7	7.950	276.8	7.202	0.99937	2019.0	2261.1	2.79	2.83
34.775	2296.7	7.950	277.2	7.212	0.99937	2054.2	2298.9	2.84	2.83
34.775	2296.7	7.952	294.5	7.163	0.99933	2062.6	2309.3	2.86	2.84
34.775	2296.7	7.946	276.5	7.202	0.99937	2039.8	2281.1	2.79	2.81
34.775	2296.7	7.948	275.1	7.204	0.99937	2023.2	2264.4	2.78	2.82
34.775	2296.7	7.946	277.0	7.197	0.99937	2031.3	2271.9	2.78	2.81
34.775	2296.7	7.949	274.8	7.210	0.99937	2031.5	2273.7	2.80	2.83
34.775	2296.7	7.948	279.0	7.191	0.99936	2020.9	2261.8	2.78	2.82
34.775	2296.7	7.943	268.7	7.233	0.99939	2075.3	2317.6	2.82	2.79
34.775	2296.7	7.946	276.9	7.194	0.99937	2021.7	2261.5	2.77	2.81
34.775	2296.7	7.942	288.6	7.170	0.99934	2078.3	2320.7	2.82	2.79
34.775	2296.7	7.943	275.6	7.200	0.99937	2041.5	2281.4	2.78	2.80
34.775	2296.7	7.943	283.2	7.174	0.99935	2037.9	2277.3	2.77	2.79

Salinity	TA	pH_1	ΔNO_3^- (µmol/Kg)	pH_2	θ	C_T (µmol/Kg)	A_{T1} (µmol/Kg)	Ω_{spec}	Ω_{calc}
34.775	2296.7	7.943	267.8	7.228	0.99939	2047.2	2287.6	2.79	2.80
34.775	2296.7	7.943	283.4	7.174	0.99935	2040.9	2280.7	2.78	2.80
34.775	2296.7	7.945	280.5	7.181	0.99936	2020.1	2259.6	2.76	2.81
34.775	2296.7	7.939	277.8	7.192	0.99936	2059.3	2298.2	2.78	2.78
34.775	2296.7	7.945	274.9	7.197	0.99937	2017.8	2256.6	2.75	2.80
34.648	2285.2	7.864	252.9	7.151	0.99942	2088.2	2288.5	2.39	2.39
34.648	2285.2	7.862	251.6	7.150	0.99942	2078.4	2277.0	2.37	2.38
34.648	2285.2	7.863	230.4	7.220	0.99947	2081.3	2280.7	2.38	2.39
34.648	2285.2	7.862	231.4	7.216	0.99947	2089.2	2288.4	2.38	2.38
34.648	2285.2	7.859	240.0	7.194	0.99945	2119.3	2319.2	2.40	2.37
34.648	2285.2	7.863	242.0	7.182	0.99945	2083.2	2282.5	2.38	2.38
34.648	2285.2	7.862	230.6	7.221	0.99947	2091.3	2291.0	2.39	2.38
34.648	2285.2	7.866	231.1	7.222	0.99947	2079.3	2280.1	2.39	2.40
34.648	2285.2	7.863	234.7	7.206	0.99946	2080.9	2280.5	2.38	2.39
34.648	2285.2	7.866	224.1	7.234	0.99949	2040.5	2238.8	2.35	2.40
34.648	2285.2	7.863	213.1	7.283	0.99951	2108.7	2309.7	2.41	2.38
34.648	2285.2	7.866	212.1	7.287	0.99952	2085.8	2287.2	2.40	2.40
34.648	2285.2	7.869	236.5	7.211	0.99946	2084.3	2287.1	2.42	2.42
34.648	2285.2	7.861	232.8	7.217	0.99947	2108.9	2309.2	2.40	2.38
34.648	2285.2	7.865	239.5	7.195	0.99945	2089.0	2289.7	2.40	2.39
34.648	2285.2	7.864	221.6	7.248	0.99949	2076.5	2275.9	2.38	2.39
Spectrophotometer 3									
34.230	2260.1	8.001	308.4	7.177	0.99930	1995.0	2260.7	3.04	3.04
34.230	2260.1	8.002	289.8	7.245	0.99934	2008.0	2275.1	3.07	3.05
34.230	2260.1	7.998	309.4	7.181	0.99930	2028.1	2295.1	3.08	3.03
34.230	2260.1	8.002	309.8	7.168	0.99930	1982.9	2247.8	3.03	3.04
34.230	2260.1	8.002	310.4	7.163	0.99930	1969.6	2233.7	3.01	3.05
34.230	2260.1	8.000	310.6	7.164	0.99930	1986.5	2250.7	3.02	3.04
34.230	2260.1	7.999	310.9	7.165	0.99930	1995.2	2259.9	3.03	3.03
34.230	2260.1	7.999	307.5	7.173	0.99930	1986.5	2250.3	3.02	3.03
34.230	2260.1	7.999	306.2	7.174	0.99931	1977.7	2240.8	3.01	3.03
34.230	2260.1	8.000	305.4	7.186	0.99931	1998.4	2263.8	3.04	3.04
34.230	2260.1	8.024	315.3	7.172	0.99931	1929.3	2202.4	3.08	3.17
34.230	2260.1	8.010	323.5	7.146	0.99930	1998.2	2269.5	3.11	3.09
34.230	2260.1	8.015	323.3	7.143	0.99930	1966.6	2237.7	3.09	3.12
34.230	2260.1	8.019	324.6	7.146	0.99929	1964.9	2238.4	3.11	3.14
34.230	2260.1	8.014	309.8	7.196	0.99933	1991.4	2264.3	3.12	3.11
34.230	2260.1	8.016	294.7	7.244	0.99936	1973.3	2245.9	3.11	3.13
34.230	2260.1	8.011	301.4	7.220	0.99934	1996.5	2268.3	3.11	3.10
34.230	2260.1	8.015	308.3	7.202	0.99933	1990.1	2263.6	3.12	3.12
34.230	2260.1	8.010	305.8	7.209	0.99934	2008.6	2281.0	3.12	3.09

Salinity	TA	pH_1	ΔNO_3^- (µmol/Kg)	pH_2	θ	C_T (µmol/Kg)	A_{T1} (µmol/Kg)	Ω_{spec}	Ω_{calc}
34.230	2260.1	8.015	303.0	7.219	0.99934	1985.0	2258.3	3.12	3.12
Spectrophotometer 4									
34.230	2260.1	8.000	279.7	7.266	0.99938	1979.7	2243.4	3.01	3.04
34.230	2260.1	8.008	313.7	7.150	0.99930	1938.9	2203.4	3.00	3.08
34.230	2260.1	7.999	318.0	7.143	0.99929	1999.4	2264.1	3.04	3.03
34.230	2260.1	7.997	321.8	7.137	0.99928	2025.8	2291.5	3.06	3.02
34.230	2260.1	7.996	302.6	7.196	0.99932	2023.6	2288.5	3.05	3.01
34.230	2260.1	7.998	318.9	7.126	0.99929	1969.8	2231.4	2.98	3.02
34.230	2260.1	7.998	303.7	7.180	0.99932	1981.8	2244.2	3.00	3.02
34.230	2260.1	7.998	305.6	7.172	0.99932	1975.6	2237.5	2.99	3.02
34.230	2260.1	7.993	308.1	7.165	0.99931	2000.4	2261.9	3.00	3.00
34.230	2260.1	7.997	297.3	7.206	0.99934	1996.8	2260.1	3.02	3.02
34.230	2260.1	8.017	298.5	7.232	0.99933	1968.3	2241.2	3.11	3.13
34.230	2260.1	8.018	310.7	7.189	0.99931	1960.8	2233.4	3.10	3.14
34.230	2260.1	8.012	315.7	7.168	0.99930	1983.0	2253.8	3.09	3.10
34.230	2260.1	8.015	297.6	7.227	0.99934	1962.3	2233.0	3.08	3.12
34.230	2260.1	8.013	311.0	7.180	0.99931	1968.4	2238.5	3.08	3.11
34.230	2260.1	8.015	303.5	7.211	0.99932	1970.4	2242.0	3.09	3.12
34.230	2260.1	8.013	284.5	7.269	0.99937	1961.7	2231.4	3.07	3.11
34.230	2260.1	8.013	278.8	7.294	0.99938	1976.1	2247.1	3.09	3.11
34.230	2260.1	8.016	314.3	7.168	0.99930	1949.2	2219.5	3.07	3.13
34.230	2260.1	8.010	298.5	7.222	0.99933	1980.7	2250.5	3.08	3.09

Appendix B: Saturation State Example Calculation

Example using meta-cresol purple (which is used for cases of $pH_1 > 7.8$)

T = 25 °C

S = 34.230

${}_{235}\varepsilon^{*}_{NO3}$ = 285.5

l = 10 cm

HNO_3 = 0.5 M

Measured pH absorbances:

	First mCP addition			**Second mCP addition**		
	${}_{434}A$	${}_{578}A$	${}_{730}A$	${}_{434}A$	${}_{578}A$	${}_{730}A$
Cell 1	0.38643	0.77099	0.00069	0.76363	1.52070	−0.00070
	0.38566	0.76908	0.00063	0.76369	1.51880	−0.00058
	0.38640	0.76986	0.00037	0.76385	1.52160	−0.00089
	0.38612	0.76981	0.00031	0.76345	1.52070	−0.00110
	${}_{434}A$	${}_{578}A$	${}_{730}A$	${}_{434}A$	${}_{578}A$	${}_{730}A$
Cell 2	0.62607	0.21225	0.00142	1.21970	0.41584	0.00073
	0.62484	0.21237	0.00119	1.21550	0.41551	0.00062
	0.62467	0.21260	0.00098	1.21630	0.41593	0.00112
	0.62418	0.21294	0.00117	1.21420	0.41645	0.00091

Measured nitrate absorbances:

	${}_{235}A$	${}_{385}A$
Cell 2	0.90239	0.001170
	0.90118	0.000745
	0.90151	0.001057
	0.90123	0.000922

1. Calculation of the initial *R* ratio (R_i) for each cell

1- Calculate the *R* for each set of absorbance measurements:

$$R = \frac{{}_{578}A - {}_{730}A}{{}_{434}A - {}_{730}A}$$

Cell 1, First mCP Addition:

$$R = \frac{0.77099 - 0.00069}{0.38643 - 0.00069}; \quad R = 1.99694$$

$$R = \frac{0.76908 - 0.00063}{0.38566 - 0.00063}; \quad R = 1.99582$$

$$R = \frac{0.76986 - 0.00037}{0.38640 - 0.00037}; \quad R = 1.99334$$

$$R = \frac{0.76981 - 0.00031}{0.38612 - 0.00031}; \quad R = 1.99452$$

2- Calculate the average *R* ratio for each addition of mCP, where

R_1 = absorbance ratio for first mCP addition

R_2 = absorbance ratio for second mCP addition

Cell 1, First mCP Addition:

$$R_1 = (1.99694 + 1.99581 + 1.99335 + 1.99452)/4$$
$$= 1.99515$$

3- Repeat for the other sets of absorbance measurements

Cell 1:

First mCP addition	**Second mCP addition**
1.99694	1.99050
1.99582	1.98801
1.99334	1.99085
1.99452	1.99045
***R*₁ = 1.99515**	***R*₂ = 1.98995**

Cell 2:

First mCP addition	**Second mCP addition**
0.33752	0.34054

0.33862	0.34151
0.33930	0.34136
0.33991	0.34249
$\boldsymbol{R_1}$ **= 0.33884**	$\boldsymbol{R_2}$ **= 0.34147**

4- Adjust for the pH perturbation caused by the indicator addition:

$$R_{\mathrm{i}} = R_1 - (R_2 - R_1)$$

Cell 1: $R_{\mathrm{i}} = 1.99515 - (1.98995 - 1.99515)$
$= 2.00035$

Cell 2: $R_{\mathrm{i}} = 0.33884 - (0.34147 - 0.33884)$
$= 0.33620$

2. Calculation of pH₁ and pH₂

1- Calculate pH using the equations from Liu et al. (2011):

$$\mathrm{pH_T} = -\log(\mathrm{K_2^T} e_2) + \log\left(\frac{R_{\mathrm{i}} - e_1}{1 - R_{\mathrm{i}}\frac{e_3}{e_2}}\right)$$

where

$e_1 = -0.007762 + 4.5174 \times 10^{-5} \cdot T$

$e_3/e_2 = -0.020813 + 2.60262 \times 10^{-4} \cdot T + 1.0436 \times 10^{-4}(S - 35)$

$-\log(\mathrm{K_2^T} e_2) = a + \frac{b}{T} + c \cdot \ln(T) - d \cdot T$

$a = -246.64209 + 0.315971 \cdot S + 2.8855 \times 10^{-4} S^2$

$b = 7229.23864 - 7.098137 \cdot S - 0.057034 \cdot S^2$

$c = 44.493382 - 0.052711 \cdot S$

$d = 0.0781344$

for $20 \leq S \leq 40$ and $278.15 \leq T \leq 308.15$K

For Cell 1: T = 298.15 K; S = 34.230; $R_{\mathrm{i}} = 2.00035$

$$\mathrm{pH_1} = 7.64903 + \log\left(\frac{2.00035 - 0.00571}{1 - 2.00035 \cdot 0.05670}\right)$$
$$= 8.0012$$

For Cell 2: T = 298.15 K; S = 34.230; $R_i = 0.33620$

$$pH_2 = 7.64903 + \log\left(\frac{0.33620-0.00571}{1-0.33620\cdot 0.05670}\right)$$
$$= 7.1766$$

*These equations apply when using mCP indicator to measure pH. If cresol red indicator is used (i.e., for cases of pH_1 <7.8), then use equations from Patsavas et al. (2013).

3. Calculation of ΔNO_3^-

1- Perform a baseline correction of the absorbances measured at 235 nm by subtracting the absorbance measured at 385 nm:

$$0.90239 - 0.001170 = 0.901220$$
$$0.90118 - 0.000745 = 0.900435$$
$$0.90151 - 0.001057 = 0.900453$$
$$0.90123 - 0.000922 = 0.900308$$

2- Calculate the average absorbance at 235 nm ($_{235}A_{NO3}$).

$$_{235}A_{NO3} = \frac{0.901220 + 0.900435 + 0.900453 + 0.900308}{4}$$
$$= 0.900604$$

3- Calculate the seawater density (ρ_{sw}) using equations from Millero and Poisson (1981):

$$\rho_{SW} = \rho_0 + AS + BS^{1.5} + CS^2$$

where

$$A = 0.824493 - 4.0899 \times 10^{-3} \cdot T + 7.6438 \times 10^{-5} \cdot T^2 - 8.2467 \times 10^{-7} \cdot T^3 + 5.3875 \times 10^{-9} \cdot T^4$$

$$B = -5.72466 \times 10^{-3} + 1.0227 \times 10^{-4} \cdot T - 1.6546 \times 10^{-6} \cdot T^2$$

$$C = 4.8314 \times 10^{-4}$$

$$\rho_o = 999.842594 + 6.793952 \times 10^{-2} \cdot T - 9.095290 \times 10^{-3} \cdot T^2 + 1.001685 \times 10^{-4} \cdot T^3 - 1.120083 \times 10^{-6} \cdot T^4 + 6.536336 \times 10^{-9} \cdot T^5$$

At T = 25 °C and S = 34.23, ρ_{sw} = 1.022743 kg L^{-1}

4- Calculate the concentration of added nitrate (ΔNO_3^-)

$$\Delta NO_3^- = \frac{{}_{235}A_{NO3}}{l \cdot {}_{235}\varepsilon_{NO3} \cdot \rho_{sw}}$$

$$\Delta NO_3^- = 0.900604/(10 \cdot 285.5 \cdot 1.022743)$$
$$= 3.08433 \times 10^{-4}\ \text{M}$$

4. Calculation of f_{B1}, f_{W1}, and f_{C1}

1- In CO2SYS, plug in *S*, *T*, *P*, pH_1, and an arbitrary $C_{T(A)}$ value as input parameters. Use K_1 and K_2 from Leuker at al., 2000; $KHSO_4$ from Dickson (1990); B_T value from Uppstrom (1974); and the total pH scale. Record the output borate alkalinity (B-Alk), hydroxide alkalinity (OH), and total alkalinity ($A_{T(A)}$).

f_{B1} = Borate Alkalinity in moles kg^{-1}

f_{W1} = Hydroxide Alkalinity in moles $kg^{-1} - [H^+]_1$

2- In CO2SYS, using the same values of *S*, *T*, *P*, and pH_1, change the C_T to another arbitrary value, $C_{T(B)}$, and record the resulting total alkalinity ($A_{T(B)}$)

$$f_{C1} = \frac{A_{T(B)} - A_{T(A)}}{C_{T\,(B)} - C_{T\,(A)}}$$

First set of CO2SYS input parameters >>>>>>>

T = 25 °C

S = 34.23

P = 0 dbars

pH_1 = 8.0012

$C_{T(A)}$ = 2000

Output:

B-Alk = 81.518 µmol kg^{-1}

OH = 5.9545 µmol kg^{-1}

$A_{T(A)}$ = 2266.12 µmol kg^{-1}

Second set of input parameters: >>>>>>>>>>

T = 25 °C

S = 34.23

P = 0 dbars

pH_1 = 8.0012

$C_{T(B)}$ = 4000

Output:

$A_{T(B)}$ = 4444.78 µmol kg^{-1}

$$f_{B1} = 81.518 \times 10^{-6}$$

$$= 8.1518 \times 10^{-5} \text{mol kg}^{-1}$$

$$f_{W1} = 5.9545 \times 10^{-6} - 10^{-8.0012}$$
$$= 5.9445 \times 10^{-6} \text{mol kg}^{-1}$$

$$f_{C1} = \frac{4444.78 - 2266.12}{4000 - 2000}$$
$$= 1.08933$$

5. Calculation of f_{B2}, f_{W2}, and f_{C2}

1- Repeat the same steps used to calculate f_{B1}, f_{W1}, and f_{C1}, but now using pH_2:

$$f_{B2} = 1.4716 \times 10^{-5}$$
$$f_{W2} = 8.2510 \times 10^{-7}$$
$$f_{C2} = 0.97067$$

6. Calculation of the dilution factor θ

For additions of 0.477 M HNO_3, the equation that relates θ to ${}_{235}A_{NO3}$ is given by

$$\theta = 1 - 0.000776 * {}_{235}A_{NO3}$$

For a different concentration of HNO_3, the slope will change by a factor of $0.477*[HNO_3]^{-1}$.

For 0.5 M HNO_3, for example:

$$\text{Slope} = -0.000776 * 0.477/0.5$$
$$= -.000740$$

$$\theta = 1 - 0.000740 * 0.90060$$
$$= 0.999334$$

7. Calculation of C_T

$$C_T = \frac{\theta^{-1}\Delta NO_3^- + f_{B2} - f_{B1} + \theta^{-1} f_{w2} - f_{w1}}{f_{C1} - f_{C2}}$$

$$C_T = \frac{3.08433\times10^{-4}\cdot0.999334^{-1}+1.4716\times10^{-5}-8.1518\times10^{-5}+8.2510\times10^{-6}\cdot0.999334^{-1}-5.9445\times10^{-6}}{1.08933-0.97067}$$

$$= 1.9949 \times 10^{-3} \text{ mole kg}^{-1}$$

8. Calculation of A_{T1}

$$A_{T1} = C_T \cdot f_{C1} + f_{B1} + f_{W1}$$

$$A_{T1} = 1.9949 \times 10^{-3} \cdot 1.08933 + 8.1518 \times 10^{-5} + 5.9445\times10^{-6}$$
$$= 2.2606 \times 10^{-3} \text{mole kg}^{-1}$$

9. Calculation of Aragonite Saturation State and other CO_2 system parameters

1- In CO2SYS, plug in *S*, *T*, *P*, C_T, and A_{T1} as input parameters, and all other CO_2 system variables will be given as output parameters:

$\Omega_{spec\text{- }arag} = 3.04$

$\Omega_{spec\text{- }cal} = 4.62$

$[CO_3^{2-}]_T = 190.9$ µmole kg^{-1}

$fCO_2 = 443.5$ µatm

$pH_1 = 8.0012$

$A_{T1} = 2260.6$ µmole kg^{-1}

$C_T = 1994.9$ µmole kg^{-1}

Appendix C: Photograph Release Form for Figure 4

Photograph Release Form
University of South Florida

I hereby allow the photo of me to be used in the electronic thesis of Erin Cuyler. I grant the University of South Florida permission to publish this thesis with my photo in any manner they wish.

Description of Shoot: In lab use of the next generation photometer
Subject's Name: _____
Legal Guardian (Name Printed): _____
Legal Guardian (Signature): _____
Date: _____